



1 **Characteristics and sources of aerosol aminiums over the eastern**
2 **coast of China: Insights from the integrated observations in a coastal**
3 **city, adjacent island and the marginal seas**

4 Shengqian Zhou¹, Haowen Li¹, Tianjiao Yang¹, Ying Chen^{*1,2}, Congrui Deng^{*1}, Yahui Gao^{3,4},
5 Changping Chen^{3,4}, Jian Xu¹

6 ¹Shanghai Key Laboratory of Atmospheric Particle Pollution Prevention, Department of Environmental Science & Engineering,
7 Fudan University, Jiangwan Campus, Shanghai 200438, China.

8 ²Institute of Eco-Chongming (IEC), 3663 N. Zhongshan Rd., Shanghai 200062, China

9 ³Key Laboratory of the Ministry of Education for Coastal and Wetland Ecosystems, School of Life Sciences, Xiamen
10 University, Xiamen 361005, China

11 ⁴State Key Laboratory of Marine Environmental Science, Xiamen University, Xiamen 361005, China

12 **Correspondence:** Ying Chen (yingchen@fudan.edu.cn) and Congrui Deng (congruideng@fudan.edu.cn)

13 **Abstract.** An integrated observation on aerosol aminiums was conducted in a coastal city (Shanghai) of eastern China, a
14 nearby island (Huaniao Island) and over the Yellow Sea and East China Sea (YECS). Triethylaminium (TEAH⁺) was the most
15 abundant aminium observed in Shanghai but not detected over the island and the open seas, suggesting its predominantly
16 terrestrial origin. By contrast, relatively high concentrations of dimethylaminium (DMAH⁺) and
17 trimethylaminium+diethylaminium (TMDEAH⁺) were measured over the ocean sites. Environmental factors, including
18 boundary layer height (BLH), temperature, atmospheric oxidizing capacity and relative humidity, were found to be related to
19 aminium concentrations. All the detected aminiums demonstrated the highest levels in winter in Shanghai, consistent with the
20 lowest BLH, temperature and oxidizing capacity in this season. Aminiums mainly existed in fine particles and showed a
21 bimodal distribution with two peaks at 0.18–0.32 μm and 0.56–1.0 μm, indicating that condensation and cloud processing were
22 primary formation pathways for aminiums. Nonetheless, a unimodal distribution for aerosol aminiums was usually measured
23 over the YECS or influenced mainly by the marine air-mass over the Huaniao Island, which was probably related to sea-spray
24 aerosols that either contained primary aminiums or provided surface for heterogeneous reactions to form secondary aminiums.
25 Terrestrial anthropogenic sources and marine biogenic sources were both important contributors for DMAH⁺ and TMDEAH⁺,
26 and the latter exhibited a significantly higher TMDEAH⁺ to DMAH⁺ ratio. By using the mass ratio of methanesulfonate (MSA)
27 to non-sea-salt SO₄²⁻ as an indicator of marine biogenic source, we estimated that marine biogenic source contributed to 57–
28 83% and 29–38% of aerosol aminiums over Huaniao Island in the summer of 2017 and autumn of 2016, respectively.

29 **1 Introduction**

30 Low molecular weight amines are commonly found in the atmosphere in both gaseous and particulate phases (Ge et al., 2011b,
31 a). Base on present theoretical calculations (Kurten et al., 2008; Loukonen et al., 2010; Paasonen et al., 2012; Olenius et al.,
32 2017), laboratory simulations (Wang et al., 2010a; Wang et al., 2010b; Kurten et al., 2014; Erupe et al., 2011; Almeida et al.,
33 2013; Yu et al., 2012) and field observations (Smith et al., 2010; Kürten et al., 2016; Tao et al., 2016), amines in the atmosphere
34 have been proved to play an important role in new particle formation and subsequent particle growth, and thus affect both the
35 number concentrations of aerosols and cloud condensation nuclei which are closely relevant to regional climate (Tang et al.,
36 2014; Yao et al., 2018). For example, dimethylamine (DMA) was found to be a key species involved in new particle formation
37 events in the urban area of Shanghai, and the nucleation mechanism was likely to be H₂SO₄-DMA-H₂O ternary nucleation
38 (Yao et al., 2018). Gaseous amines in the atmosphere can react with oxidants such as ·OH and O₃ to form secondary organic
39 aerosols (SOA) (Murphy et al., 2007) or other gases (Nielsen et al., 2012). The heterogeneous reaction, such as replacing the



40 NH_4^+ in particles, is another important pathway for amines to form SOA in the atmosphere (Pankow, 2015; Kupiainen et al.,
41 2012; Liu et al., 2012; Chan and Chan, 2013). In aerosols, amines are mainly in the form of protonated cations, namely
42 aminiums (Ge et al., 2011a).

43 Amines originate from a wide range of sources, including anthropogenic sources such as animal husbandry and industrial
44 emissions, as well as natural sources such as marine sources, vegetation emissions, and soil processing, etc. (Ge et al., 2011b;
45 Hemmilä et al., 2018). Zheng et al. (2015) measured amines in a suburban site of Nanjing in China, and concluded that amines
46 and NH_3 in the region were mainly from industrial emissions in adjacent areas. Shen et al. (2017) demonstrated that coal
47 combustion could emit abundant methylaminium (MMAH^+), ethylaminium (MEA^+) and diethylaminium (DEAH^+) through
48 combustion experiments, and the corresponding emission factors were 18.0 ± 16.4 , 30.1 ± 25.6 and 14.6 ± 10.1 mg kg^{-1} ,
49 respectively. In marine boundary layer, marine source is an important contributor for amines and it is closely related to marine
50 surface biological activities. In the North Atlantic, the concentrations of dimethylaminium (DMAH^+) and DEAH^+ were
51 significantly higher during the periods with high biological activity and clean air-mass conditions than those with low
52 biological activity or polluted air masses advecting to the sampling site, and the contributions of these two aminiums to SOA
53 and water soluble organic nitrogen (WSO) reached 11% and 35%, respectively (Facchini et al., 2008). The observation in
54 Cape Verde also showed that the concentrations of amines were higher during the occurrence of algal blooms (Müller et al.,
55 2009). Previous studies on aminiums over the marginal seas of China indicated that DMAH^+ and trimethylaminium (TMAH^+)
56 were overwhelmingly from marine sources (Hu et al., 2015; Yu et al., 2016; Xie et al., 2018). In May 2012, the concentrations
57 of DMAH^+ and TMAH^+ over the Yellow Sea (YS) and Bohai Sea even reached 4.4 ± 3.7 and 7.2 ± 7.1 nmol m^{-3} , which was 1–
58 3 orders of magnitude higher than those reported in other oceanic regions (Hu et al., 2015). These extremely high
59 concentrations were thought to be associated with high biological activities.

60 Given the potentially important roles of amines in the atmosphere and the complexity of their sources, it is important to conduct
61 a systematic analysis on their concentrations, affecting factors, formation pathways and source contributions. The eastern
62 China is a densely populated region with strong human activities and large emissions of atmospheric pollutants. Under the
63 influence of the summer monsoon, marine source components can be vital to the atmospheric composition of the coastal area.
64 Although the lifetime of gaseous amines in the atmosphere is only a few hours, it can be prolonged after amines partition into
65 the particulate phase, and thus, they may be transported over a long range (Nielsen et al., 2012). Many studies have been done
66 on the atmospheric amines over eastern China and adjacent seas (Huang et al., 2012; Hu et al., 2015; Zheng et al., 2015; Huang
67 et al., 2016; Tao et al., 2016; Yu et al., 2016; Shen et al., 2017; Xie et al., 2018; Yao et al., 2018; Yao et al., 2016). Nonetheless,
68 the long-term observation of aminiums over the coastal sea and quantitative estimate of the contribution of marine biogenic
69 source to aerosol aminiums are still lacking.

70 In this study, the aminiums over a coastal megacity (Shanghai), a nearby island (Huaniao Island) and marginal seas (the Yellow
71 Sea and East China Sea, YECS) were measured. The relationships between aminium concentrations and environmental factors
72 were systematically analyzed. The size distributions of aminiums were investigated with the speculation of primary formation
73 pathways. Besides, the dominant sources determining the concentrations and ratios between aminium species were elucidated,
74 and the contributions of terrestrial anthropogenic and marine biogenic sources to aminiums were quantitatively estimated. Our
75 results will be a great help for understanding the chemical properties, reaction pathways and sources of aerosol aminiums over
76 the coastal area and the ocean.

77 2 Sampling and Analysis

78 2.1 Aerosol sampling

79 The sampling site in Shanghai was located on top of the No.4 teaching building of Fudan University (31.30° N, 121.50° E)
80 (Fig. 1). This site is affected by the school, residential, commercial and traffic activities and can be a representative of coastal



81 cities. Particulate matters with an aerodynamic diameter less than 2.5 μm ($\text{PM}_{2.5}$) were simultaneously collected by two
82 medium-flow samplers (100 L min^{-1} , HY-120B, Hengyuan) using a 90 mm pre-combusted quartz filter (Whatman) and a
83 cellulose filter (Grade 41, Whatman), respectively. A total of 131 samples were collected within four seasons with the sampling
84 duration \sim 24 hours (Table 1).

85 Aerosols were also collected at Huaniao Island (HNI, 30.86° N, 121.67° E) which was about 80 km away from Shanghai in
86 the East China Sea (ECS) (Fig. 1). The locally anthropogenic emissions were negligible, but the site was affected by the
87 terrestrial transport and the ship emission from nearby container ports (Wang et al., 2016; Wang et al., 2018). Fourteen $\text{PM}_{2.5}$
88 samples were collected in the summer of 2016 and size-segregated samples were obtained using a 10-stage Micro-Orifice
89 Uniform Deposit Impactor (30 L min^{-1} , MOUDI, MSP Model 110-NR) and 47 mm PTFE filters (Zeflour, PALL) between 2016
90 fall and 2017 late summer (Table 1). The 50% cutoff diameters for 10 stages were 18, 10, 5.6, 3.2, 1.8, 1.0, 0.56, 0.32, 0.18,
91 0.10 and 0.056 μm , and the sampling durations were 24–48 hours.

92 The size-segregated samples were also collected over the YECS onboard research vessel (R/V) *Dong Fang Hong II* in the
93 spring of 2017. The cruise started from Qingdao on March 27 and returned on April 15 (Fig. 1), and a total of 9 sets of samples
94 were obtained.

95 2.2 Chemical analysis

96 One fourth of $\text{PM}_{2.5}$ sample and half of MOUDI sample filters were cut and placed into a polypropylene jar (Nelgene) with 20
97 mL of ultrapure water (18.25 $\text{M}\Omega\text{ cm}^{-1}$) for 40 min ultrasonic extraction. The extract was filtered through a 0.45 μm PTFE
98 filter (Jinteng) and stored at 4 °C for ion measurement. Ion Chromatograph (DIONEX ICS-3000, Thermo-Fisher) assembled
99 with AG11-HC and AS11-HC was used to determine anions including Cl^- , NO_3^- , SO_4^{2-} , HCOO^- , methanesulfonate (MSA),
100 malonate, succinate, glutarate, maleate and $\text{C}_2\text{O}_4^{2-}$. The columns CG17 and CS17 were used to measure inorganic cations
101 including Na^+ , NH_4^+ , K^+ , Mg^{2+} and Ca^{2+} and aminiums. The detailed procedures for measuring DMAH^+ , TMAH^+ + DEAH^+ ,
102 propylaminium (MPAH⁺), triethylaminium (TEAH⁺), ethanolaminium (MEOAH⁺) and triethanolaminium (TEOAH⁺) refer to
103 Zhou et al. (2018). It should be noted that TMAH^+ and DEAH^+ could not be completely separated using the IC system
104 (VandenBoer et al., 2012; VandenBoer et al., 2011; Zhou et al., 2018; Huang et al., 2014). Nonetheless, the sum of TMAH^+
105 and DEAH^+ concentrations (referred to TMDEAH^+) might be quantified using the calibration curve of TMAH^+ with errors
106 less than 3% (Zhou et al., 2018).

107 One fourth of $\text{PM}_{2.5}$ cellulose sample filter was cut and digested with 7 mL of HNO_3 and 1 mL of HF (both acids were purified
108 from GR using a sub-boiling system) at 185 °C for 30 min in a microwave digestion system (MARSS Xpress, CEM). An
109 Inductively Coupled Plasma Optical Emission Spectroscopy (ICP-OES, SPECTRO) was used for determining elements Al,
110 Ca, Fe, Na, P, S, Cu, K, Mg, Mn, Zn, As, Ba, Cd, Ce, Co, Cr, Mo, Ni, Pb, Ti, and V. The detailed procedures refer to Wang et
111 al. (2016).

112 2.3 Auxiliary data

113 The 3-hour resolution meteorological data of Baoshan station in Shanghai (WMO index: 58362) were obtained from the
114 National Climatic Data Center (NCDC, <https://www.ncdc.noaa.gov/isd>). The 10-second resolution meteorological data were
115 recorded by a shipborne meteorological station during the cruise. The planetary boundary layer height (BLH) and 6-hour
116 accumulated precipitation (TPP6) for the cruise were extracted from NCEP's Global Data Assimilation System Data (GDAS).
117 The daily concentrations of gaseous pollutants (SO_2 , CO, NO_2 and O_3) in Shanghai were obtained from the Shanghai
118 Environmental Monitoring Center (<http://www.semcc.gov.cn/aqi/home/DayData.aspx>).

119 Three-day air mass backward trajectories were calculated using a Hybrid Single-Particle Lagrangian Integrated Trajectory
120 (HYSPPLIT) model (<http://ready.arl.noaa.gov/HYSPLIT.php>) with the starting height at 100 meters.



121 **3 Results and discussion**

122 **3.1 Seasonal and spatial variations of aminium concentrations**

123 Three aminiums, DMAH⁺, TMDEAH⁺ and TEAH⁺, were commonly detected in the aerosol samples collected from Shanghai.
124 The most abundant aminiums were DMAH⁺ and TEAH⁺ with their annual means of 15.6 and 16.0 ng m⁻³, respectively. By
125 comparison, the average TMDEAH⁺ concentration (4.4 ng m⁻³) was significantly lower. All three aminiums showed the highest
126 concentrations in winter and the lowest levels in spring (DMAH⁺) and summer (TMDEAH⁺ and TEAH⁺), which generally
127 agreed with the seasonal trends of PM_{2.5} and NH₄⁺ concentrations in Shanghai (Figure 2). Specifically, the average TEAH⁺
128 reached 35.2 ng m⁻³ in winter in Shanghai, about 40 times as much as that in summer. By contrast, TEAH⁺ was mostly below
129 the detection limit in the aerosols collected over Huaniao Island and the YECS, suggesting its dominant land sources and
130 negligible marine contribution. Differently, the average DMAH⁺ and TMDEAH⁺ concentrations (14.0 and 13.2 ng m⁻³) over
131 Huaniao Island were close to and significantly higher than those of Shanghai, respectively. Similarly high concentrations of
132 DMAH⁺ and TMDEAH⁺ (11.9 and 14.6 ng m⁻³) were also observed over the YECS (Fig. 2 and Table 2), suggesting that the
133 two aminiums might have notable marine sources. Accordingly, both species reached the highest levels during the summer
134 campaigns in 2017 at Huaniao Island, consistent with the highest primary productivity in the coastal ECS and prevailing winds
135 from the ocean in summer. As a major component of fine particles over eastern China with similar chemical properties to
136 aminiums, NH₄⁺ was mainly from terrestrial sources and its concentrations over Huaniao Island were much lower than those
137 over Shanghai (Fig. 2).

138 Our measurement of DMAH⁺ in Shanghai was comparable to those previously reported from the urban sites (Table 2), but
139 generally higher than those measured in the forest areas of Toronto (VandenBoer et al., 2012), Hyytiälä (Hemmilä et al., 2018)
140 and Guangdong (Liu et al., 2018a). This implies that anthropogenic activities may be crucial sources of DMAH⁺ in the urban
141 atmosphere. The TMDEAH⁺ concentrations in our study were much lower than those reported by Tao et al. (2016) in Shanghai.
142 Their sampling location was close to the residential areas and could be influenced by the local sources such as human excreta
143 emission (Zhou et al., 2018). The aerosol TEAH⁺ concentrations in China were firstly reported in our study and could not be
144 compared to previous work. Except for the three aminiums, MMAH⁺ and MEAH⁺ (Liu et al., 2018a; Ho et al., 2015; Shen et
145 al., 2017) were other abundant aminiums detected in the urban site.

146 Aerosols were sampled using a MOUDI over Huaniao Island and the YECS. Aminiums in PM_{1.8} of the MOUDI samples were
147 compared to those of PM_{2.5}, since MOUDI does not have the 50% cutoff diameter of 2.5 μm and aminiums in PM_{1.8} accounted
148 for over 60% concentrations of the whole size range of aerosols. Our measurements of aminiums over Huaniao Island and the
149 YECS were comparable to those previously observed over the eastern China seas (Hu et al., 2015; Yu et al., 2016; Xie et al.,
150 2018), but they were apparently higher than many other oceanic regions such as Arabian Sea (Gibb et al., 1999) and Cape
151 Verde (Müller et al., 2009). The high aminiums over the YECS were probably associated with the severe air pollution in eastern
152 China as well as the high ocean productivity in marginal seas.

153 **3.2 Environmental factors affecting aminium concentrations**

154 **3.2.1 Boundary layer height (BLH)**

155 The concentrations of PM_{2.5}, NH₄⁺ and three aminiums sampled in Shanghai in 2013 dropped significantly when the BLH
156 increased from 200 m to 500 m and then slowly decreased with the further increase of BLH (Fig. 3a and Fig. S1), due to the
157 improvement of diffusion condition. Specifically, the concentrations of DMAH⁺, TMDEAH⁺ and TEAH⁺ (58.4, 13.9 and 80.5
158 ng m⁻³) in Shanghai reached the maximum along with PM_{2.5} (447 μg m⁻³) during the severe haze event between 30 Nov. and 8
159 Dec. 2013, when the average BLH and wind speed were 298 m and 1.35 m s⁻¹, respectively (Fig. S2). By comparison, the
160 average concentrations of DMAH⁺, TMDEAH⁺ and TEAH⁺ (8.9, 4.0 and 10.1 ng m⁻³) were much lower prior to the haze event
161 (on 26-29 Nov 2018) associated with the higher BLH (636.4 m) and wind speed (2.73 m s⁻¹). Thus, the generally poor diffusion



162 condition in winter (Liu et al., 2013) could cause a substantial increase of aminiums in aerosols and lead to the seasonal
163 variation of aminiums in Shanghai.

164 3.2.2 Temperature

165 To eliminate the synchronous change of aminiums and NH_4^+ with $\text{PM}_{2.5}$, the mass ratios of aminiums to $\text{PM}_{2.5}$ (aminiums/ $\text{PM}_{2.5}$)
166 and NH_4^+ to $\text{PM}_{2.5}$ ($\text{NH}_4^+/\text{PM}_{2.5}$) were applied for analysis. These ratios were found to be negatively correlated with air
167 temperature in Shanghai (Fig. 3b). Similar to NH_4^+ , aminiums combined with NO_3^- , Cl^- and organic acids are semi-volatile
168 and can dissociate in the atmosphere (Tao and Murphy, 2018). So the negative correlations may be explained by the movement
169 of gas-particle partitioning equilibrium to the gas phase at higher temperatures (Ge et al., 2011a). This is consistent with the
170 previous observation that the proportion of particles containing aminiums in the urban area of Shanghai was much higher in
171 winter (23.4%) than that in summer (4.4%) (Huang et al., 2012). The seasonal variation of temperature may also lead to the
172 change of concentrations of aerosol aminiums.

173 3.2.3 Oxidizing capacity

174 As gaseous amines can be oxidized by oxidants such as $\cdot\text{OH}$, O_3 and $\text{NO}_3\cdot$ in the atmosphere before partitioning into the
175 particulate phase (Ge et al., 2011b; Nielsen et al., 2012; Yu and Luo, 2014), aminium concentrations in aerosols may decrease
176 with the enhanced atmospheric oxidizing capacity. Ozone concentration can represent oxidizing capacity of the lower
177 atmosphere (Thompson, 1992). Here the relationship between aminium/ NH_4^+ ratios and O_3 was examined, because the
178 formation of particulate aminiums and NH_4^+ were both temperature-dependent and using their ratios could avoid the
179 temperature effect to some extent. Besides, the residence time of NH_3 in the atmosphere due to the oxidation reaction is about
180 72.3 days (Ge et al., 2011b), and therefore NH_4^+ concentrations in aerosols should not be affected by O_3 . A negative correlation
181 was found between the $\text{TEAH}^+/\text{NH}_4^+$ and O_3 concentrations in Shanghai (Fig. 3c). Differently, the $\text{DMAH}^+/\text{NH}_4^+$ and
182 $\text{TMDEAH}^+/\text{NH}_4^+$ reached the highest values at the mid-level O_3 and decreased with both low and high concentrations of O_3 .
183 This verifies that high oxidizing capacity may reduce the formation of particulate aminiums by oxidizing gaseous amines. This
184 also implies that DMAH^+ and TMDEAH^+ may have the sources different from TEAH^+ but similar to O_3 precursors such as
185 biogenic VOCs. Among the three amines, the rate constants of TEA reacting with $\cdot\text{OH}$ and O_3 were larger than those of other
186 two amines (Nielsen et al., 2012), and thereby TEAH^+ showed the most significant correlation with O_3 . In general, atmospheric
187 oxidizing capacity was the strongest in summer (Logan, 1985; Liu et al., 2010), which could be another reason for seasonal
188 variation of aerosol aminiums in Shanghai.

189 In the spring of 2017 over the YECS, the concentrations of DMAH^+ and TMDEAH^+ were found to be the lowest between 29
190 Mar and 4 Apr when it was sunny and Chl-a concentrations were relatively low. The relatively low biogenic emission may
191 partly account for the low-level aminiums. Nonetheless, the HCOO^- in aerosols, a product of photochemical reactions under
192 high oxidizing capacity (Souza, 1999; Tsai et al., 2013), reached the highest level between 31 Mar. and 4 Apr. (42.1–55.5 ng
193 m^{-3}). Its concentrations were inversely correlated with aminiums when eliminating the lowest values of HCOO^- (Fig. 4). This
194 further suggests that high oxidizing capacity may be one of causes for lowered aminiums in marine aerosols.

195 3.2.4 Relative humidity and fog processing

196 In the spring of 2017 over the YECS, although the sample of 4–5 Apr. was influenced by high Chl-a concentrations and low
197 BLH, the concentrations of DMAH^+ and TMDEAH^+ (13.3 and 17.4 ng m^{-3}) were about half of those on 7–9 Apr. (Fig. 5). This
198 was probably due to the intense fog event occurred on 7–9 Apr. with relative humidity >90%, which could enhance the gas-to-
199 particle partitioning of amines. The enhancement of TMA gas to particles by cloud and fog processing has been observed in
200 both field and laboratory simulations (Rehbein et al., 2011). It was also found that the number fraction of TMA-containing
201 particles dramatically increased from ~7% in clear days to ~35% in foggy days and number-based size distribution of TMA-



202 containing particles shifted towards larger mode, peaking at the droplet mode (0.5–1.2 μm) in Guangzhou (Zhang et al., 2012).
203 The investigation over the Yellow and Bohai seas in the summer of 2015 found significantly positive correlations between the
204 concentrations of DMAH⁺ and TMAH⁺ and relative humidity (Yu et al., 2016). Therefore, high relative humidity and fog event
205 may lead to an increase of aminiums in marine aerosols.

206 3.3 Size distributions and formation pathways of aerosol aminiums

207 The aminiums were mainly distributed in fine aerosols with diameter less than 1.8 μm , and the mass percentages of DMAH⁺
208 and TMDEAH⁺ in the coarse mode were around 36% in the autumn of 2016 at Huaniao Island and less than 15% in all other
209 campaigns at Huaniao Island and over the YECS (Fig. 6a-d). The aminiums mostly demonstrated a bimodal distribution in the
210 autumn and early summer campaigns at Huaniao Island with peaks at 0.18–0.32 μm (condensation mode) and 0.56–1.0 μm
211 (droplet mode). This is similar to the size distributions of DMAH⁺ and TMDEAH⁺ observed in Shanghai (Tao et al., 2016) and
212 to NH₄⁺ and non-sea-salt (nss-SO₄²⁻) in all campaigns over Huaniao Island and the YECS (Fig. S3-4). The size distribution
213 suggests that the gas-to-particle condensation (condensation mode) and cloud processing (droplet mode) seem to be primary
214 mechanisms for the formation of aminiums and other secondary species NH₄⁺ and nss-SO₄²⁻.

215 In order to compare the contributions between condensation and cloud processing to the formation of specific species, the ratio
216 of its concentrations in droplet mode (0.56–1.0 μm) to condensation mode (0.18–0.32 μm) was calculated (denoted as α). It
217 could be seen that the α values of NH₄⁺ and nss-SO₄²⁻ were significantly greater than 1, especially in the case of high
218 concentrations, indicating that the cloud processing probably determined the concentrations of these species (Fig. 7).
219 Differently, aminiums had α values around 1, suggesting that condensation and cloud processing might be equally important
220 to the formation of aminiums.

221 In late summer at Huaniao Island and the spring cruise over the YECS when air masses were mainly from oceanic regions (see
222 Sect. 3.4.3), the aminiums generally exhibited a unimodal distribution with one wide peak at 0.18–1.0 μm due to the increased
223 concentrations at 0.32–0.56 μm (Fig. 6e-h). The concentrations of NH₄⁺ and nss-SO₄²⁻ also showed a significant elevation in
224 the size range of 0.32–0.56 μm during these periods. The deviation of MOUDI cutoff diameters during the sampling could be
225 ruled out because the concentrations of particulate matter always presented a trimodal distribution with peaks at 0.18–0.32 μm ,
226 0.56–1.8 μm and 3.2–10 μm . The unimodal distributions of aminiums with the peak at 0.18–1.0 μm have been widely reported
227 over the eastern China seas (Hu et al., 2015; Yu et al., 2016; Xie et al., 2018). This suggests that the formation mechanisms of
228 aerosol aminiums over the ocean may be different from that in the urban area. It was indicated that the high concentration and
229 unique size distribution of TMAH⁺ observed over the oligotrophic western North Pacific were mainly attributed to the primary
230 TMAH⁺ in sea-spray aerosols (Hu et al., 2018). So we speculate that the elevated concentrations of aminiums at 0.32–0.56 μm
231 over the eastern China seas may be also associated with the increased concentration of sea-spray aerosols which contain
232 substantial primary aminiums or provide more surface for heterogeneous reactions to form secondary aminiums (Yu et al.,
233 2016).

234 3.4 Sources of aerosol aminiums

235 3.4.1 Anthropogenic sources on land

236 Correlation analysis was carried out between aminiums, other PM_{2.5} components and gaseous pollutants measured in Shanghai
237 (Fig. 8). It can be seen that the secondary inorganic components SO₄²⁻, NO₃⁻ and NH₄⁺ (SNA), PM_{2.5} and DMAH⁺ were
238 significantly correlated with each other with the correlation coefficients above 0.6. This suggests that anthropogenic sources
239 may have a great contribution to the atmospheric DMA in Shanghai. The correlations between TEAH⁺ and SNA were relatively
240 weak, but TEAH⁺ was found to be significantly correlated with the components mainly from industrial sources (represented
241 by the high concentrations of K, Mn, Cd, Pb, Zn, and Cl⁻) (Tian et al., 2015; Liu et al., 2018b), indicating that the industrial



242 emission could be an important source of TEA. Compared to the DMAH⁺ and TEAH⁺, TMAH⁺ showed much weaker
243 correlations with the anthropogenically derived components. Weak correlations were also found between all the aminiums and
244 V, Ni, Al, Mg, Ca and Fe, suggesting that ship emission (traced by V and Ni) and soil dust (represented by Al, Ca and Fe) were
245 not main sources of aminiums in PM_{2.5} over Shanghai.

246 3.4.2 Marine biogenic source

247 As discussed in Sect. 3.1, the relatively high concentrations of DMAH⁺ and TMDEAH⁺ over Huaniao Island and the YECS
248 implied that the marine sources contributed substantially to these two aminiums. Accordingly, a spatial variation of aminium
249 concentrations was observed over the YECS during the spring cruise. The concentrations of DMAH⁺ and TMDEAH⁺ increased
250 by a fold of 3–5 in the southern ECS (average 24.4 and 40.3 ng m⁻³ for the samples of 7–11 Apr. respectively) compared to the
251 YS and northern ECS (average 7.0 and 8.4 ng m⁻³ for the samples of 27 Mar.–5 Apr. respectively) (Fig. 9). This is consistent
252 with the noticeable difference of Chl-a concentrations between the southern and northern YECS (2.3 folds higher in southern
253 YECS than that in northern YECS, unpublished data). Furthermore, the highest TMDEAH⁺ and lowest NH₄⁺ concentrations
254 observed on 7–11 Apr. corresponded to the air-mass back trajectories originating from the ocean, suggesting that the metabolic
255 activities of surface plankton in the high-productive seas could be a strong source of amines as previously reported (Facchini
256 et al., 2008; Müller et al., 2009; Sorooshian et al., 2009; Hu et al., 2015). Differently, the high concentrations of aminiums
257 observed on 14 Apr. near Qingdao was affected by the air masses transported from eastern China (Fig. 9) and thereby
258 contributed mainly by terrestrial sources.

259 Fine-mode NH₄NO₃ could decompose during its transport from the land to the ocean, and the released HNO₃ gas would react
260 with dust and sea salt aerosols to form coarse-mode NO₃⁻. Therefore, negative correlations were observed between the
261 concentrations of fine-mode NO₃⁻ and alkaline species (Na⁺+Ca²⁺) over the East Asia (Bian et al., 2014; Uno et al., 2017).
262 Since only one dust event was encountered on 12–13 Apr. during the cruise (unpublished data), the coarse-mode NO₃⁻ in this
263 study should be mostly formed by the heterogeneous reaction with sea salts. Therefore, the importance of terrestrial transport
264 to marine aerosols could be roughly estimated by the percentage of NO₃⁻ in the fine mode. For aerosols collected on 29–31
265 Mar., 4–5 Apr., 7–9 Apr. and 9–11 Apr., over 2/3 concentrations of NO₃⁻ were in the coarse mode (>1.8 μm, Fig. 10a). These
266 samples should be less affected by the terrestrial air masses (referred to category 1) compared to other samples (referred to
267 category 2), and the judgment was consistent with the pointing directions of back trajectories (Fig. S5). Aminiums were
268 negatively correlated with NH₄⁺ for Category 1 samples suggesting that aminiums were probably dominated by marine
269 biogenic sources whereas NH₄⁺ was influenced by terrestrial transport (Fig. 10b). For Category 2 samples, a positive
270 correlation was found between aminiums and NH₄⁺, indicating that terrestrial sources could contribute significantly to
271 aminiums over the YECS in these cases (Fig. 10c).

272 3.4.3 Source contributions to aminiums over the coastal sea

273 Huaniao Island is located in the frontline of terrestrial transport to the ECS and influenced by the air masses from the land or
274 ocean depending on the seasonal variation of prevailing winds. Significantly positive correlations were found between the
275 concentrations of aminiums and NH₄⁺ in the autumn but not in the summer of 2016 or in late summer of 2017 (Fig. 11).
276 Accordingly, the majority of backward trajectories pointed to the northern China in autumn whereas air masses predominantly
277 originated from the ECS in summer (Fig. 12). Meanwhile, NO₃⁻ demonstrated a tri-modal distribution with three peaks at
278 0.18–0.32 μm (condensation mode), 0.56–1.0 μm (droplet mode) and 3.2–5.6 μm (coarse mode) in autumn but only one peak
279 at 3.2–5.6 μm in late summer of 2017 (Fig. S6). These implies that terrestrial transport could be a dominant source for aminiums
280 over the coastal ECS in autumn while marine sources were dominant in late summer. In early summer of 2017, the mass ratios
281 of aminiums to NH₄⁺ were significantly lower on 26–28 Jun. than on other days (Fig. S7), corresponding to different origins
282 and properties of the air masses. Removing the data measured on 26–28 Jun., we found a significantly positive correlation



283 between the concentrations of DMAH⁺ and NH₄⁺ but not between TMDEAH⁺ and NH₄⁺. This suggests that DMAH⁺ and
 284 TMDEAH⁺ may be predominantly derived from terrestrial and marine sources, respectively.

285 Good positive correlations were generally found between the concentrations of TMDEAH⁺ and DMAH⁺ over Huaniao Island
 286 and the YECS, and the slope for autumn samples dominated by terrestrial sources was significantly lower than those influenced
 287 primarily by marine air masses (e.g. late summer at Huaniao Island and spring over the YECS, Fig. 13). The highest slope of
 288 TMDEAH⁺ vs DMAH⁺ (1.98) occurred in the summer of 2016 which was also mainly affected by marine sources. Therefore,
 289 it is speculated that aminiums derived from marine biogenic source might have significantly higher TMDEAH⁺ to DMAH⁺
 290 ratios than those from terrestrial sources. Similarly, Hu et al. (2015) observed a significant correlation between the TMDEAH⁺
 291 and DMAH⁺ concentrations over the Yellow Sea with the slope of 1.27–2.49. In early summer of 2017, the weak correlation
 292 between the DMAH⁺ and TMDEAH⁺ and very low slope (0.29) suggested the mixing of terrestrial and marine influence on
 293 aminiums over Huaniao Island during that period as discussed above.

294 The dimethylsulfide (DMS) produced in seawater by the metabolism of plankton will be released into the atmosphere, and
 295 SO₂, MSA, SO₄²⁻ and other products can be formed through a series of oxidation reactions (Saltzman et al., 1985; Charlson et
 296 al., 1987; Faloon, 2009; Barnes et al., 2006). MSA is often used as a tracer of marine biogenic source to calculate the marine
 297 biogenic contribution to nss-SO₄²⁻ (Yang et al., 2009; Yang et al., 2015). Therefore, the mass ratio of MSA to nss-SO₄²⁻
 298 (MSA/nss-SO₄²⁻) can be used to indicate the contribution of marine sources to aerosol components. A significantly linear
 299 relationship was found between aminium/NH₄⁺ and MSA/nss-SO₄²⁻ for the samples collected in the autumn of 2016 and
 300 summer of 2017 over Huaniao Island (Fig. 14). The value of aminium/NH₄⁺ increased with the increasing contribution of
 301 marine sources to the aminium. When the marine biogenic source contribution is 0, the corresponding aminium/NH₄⁺ values
 302 (*b* in Eq. (3)) represent the average ratios completely contributed by terrestrial sources. By multiplying the ratios by NH₄⁺
 303 concentrations, the aminiums contributed by terrestrial sources can be calculated (Eq. (4)). Therefore, the contributions of
 304 terrestrial and marine sources to aerosol aminiums can be quantitatively estimated.

305
$$([\text{aminium}]/[\text{NH}_4^+])_{\text{terrestrial}} = k \times ([\text{MSA}]/[\text{nss} - \text{SO}_4^{2-}])_{\text{terrestrial}} + b \quad (3)$$

306
$$[\text{aminium}] = ([\text{aminium}]/[\text{NH}_4^+])_{\text{terrestrial}} \times [\text{NH}_4^+] + [\text{aminium}]_{\text{marine}} \quad (4)$$

307 where *k* and *b* are the slope and intercept of the linear fitting equation of [aminium]/[NH₄⁺] and [MSA]/[nss - SO₄²⁻],
 308 respectively (Fig. 14).

309 Although most of MSA comes from marine sources, the terrestrial sources may also have a certain contribution (Yuan et al.,
 310 2004). Therefore, MSA/nss-SO₄²⁻=0 was not used as the end member value for calculating the terrestrial contribution. In winter,
 311 due to the prevailing northwest monsoon and low marine biogenic activities at low temperature, the aerosol components over
 312 Huaniao Island were overwhelmingly affected by terrestrial transport. We conducted total suspended particles (TSP) sampling
 313 in the winters of both 2014 and 2015 and obtained a total of 41 values of MSA/nss-SO₄²⁻ which were between 0.0010 and
 314 0.0068. The smallest 5 values were considered to represent the situations completely contributed by terrestrial sources, with
 315 an average 0.0018±0.0007. Substituting it into the previous fitting equation, the values of $([\text{DMAH}^+]/[\text{NH}_4^+])_{\text{terrestrial}}$ and
 316 $([\text{TMDEAH}^+]/[\text{NH}_4^+])_{\text{terrestrial}}$ were 0.0062 (0.0044–0.0093) and 0.0028 (0.0008–0.0052), respectively. Then the average
 317 contributions of terrestrial and marine sources to the two aminiums in each campaign were calculated and shown in Table 3.

318 It can be seen that the average terrestrial contributions to DMAH⁺ and TMDEAH⁺ were both more than 60% in autumn, higher
 319 than those in summer. The contributions of marine sources during late summer of 2017 (66.5% for DMAH⁺ and 82.5% for
 320 TMDEAH⁺) were higher than those in early summer (57.3% for DMAH⁺ and 79.1% for TMDEAH⁺), which was consistent
 321 with previous speculation. Furthermore, the contribution of marine sources was greater to TMDEAH⁺ than to DMAH⁺ in all
 322 campaigns, which corresponded to the higher ratio of TMDEAH⁺/DMAH⁺ in the samples influenced primarily by marine air
 323 masses (Fig. 13). It should be pointed out that although NH₄⁺ was mainly derived from the land, marine sources may also had
 324 a certain contribution (Altieri et al., 2014; Paulot et al., 2015). This was neglected in our calculation and might lead to the
 325 overestimate of terrestrial contributions to aminiums. Besides, the relatively small number of data points used in the fitting (25



326 points) and the treatment of ($[aminium]/[NH_4^+]_{terrestrial}$) as a fixed value ignoring its variation would cause uncertainty in
327 the results. Nonetheless, this is the first quantitative estimate of the contributions of terrestrial and marine sources to aerosol
328 aminiums over the coastal ECS, and the method using MSA/nss-SO₄²⁻ as an indicator of marine source is rational and feasible.

329 4 Conclusion

330 Amines in the atmosphere play an important role in new particle formation and subsequent particle growth, and studying
331 aerosol aminiums can provide insight into the sources, reaction pathways and environmental effects of amines. An integrated
332 observation was conducted on aerosol aminiums mainly DMAH⁺, TMDEAH⁺ and TEAH⁺ in a coastal city (Shanghai), a nearby
333 island (Huaniao) and the marginal seas (the YECS). All three aminiums exhibited significantly seasonal variation in Shanghai
334 with their highest concentrations in winter, which was consistent with relatively severe air pollution associated with the winter
335 monsoon (continental winds) and the lowest BLH and temperature in this season. Atmospheric oxidizing capacity and
336 relatively humidity may also influence the concentrations of aerosol aminiums to some extent by oxidizing gaseous amines
337 and enhancing the gas-particle partitioning, respectively. By comparing the ocean sites to Shanghai, similar concentrations of
338 DMAH⁺ and 3-fold higher TMDEAH⁺ were observed suggesting that these two aminiums may have significant marine sources.
339 Differently, TEAH⁺ was most abundant aminium in Shanghai but it was below the detection limit over Huaniao Island and the
340 YECS, implying its terrestrial origin.

341 Aminiums influenced substantially by terrestrial transport showed a bimodal distribution with two peaks at 0.18–0.32 μm
342 (condensation mode) and 0.56–1.0 μm (droplet mode), suggesting that the gas-to-particle condensation and cloud processing
343 were primary formation pathways for aerosol aminiums. Nonetheless, aminiums demonstrated a unimodal distribution with a
344 wide peak at 0.18–1.0 μm over the YECS and in late summer of Huaniao Island, and the elevated concentration at 0.32–0.56
345 μm might be related to sea-spray aerosols that either contain primary aminiums or provide surface for heterogeneous reactions
346 to form secondary aminiums. This indicates that aminiums in marine aerosols may undergo different formation pathways from
347 those on land.

348 We firstly distinguished the contributions of terrestrial and marine sources to aerosol aminiums by taking the mass ratio of
349 MSA to nss-SO₄²⁻ as an indicator of marine biogenic sources. In the autumn of 2016, the contributions of terrestrial sources to
350 aminiums over Huaniao Island were estimated to be more than 60%. In contrast, marine biogenic sources dominated aminium
351 concentrations especially for TMDEAH⁺ (~80%) in the summer of 2017. The proposed quantitative estimates may be helpful
352 for simulating the source emissions of amines in atmospheric chemistry models in the coastal area.

353
354 *Data availability.* Data are available from the corresponding author on request (yingchen@fudan.edu.cn).

355
356 *Author contribution.* SZ, YC and CD conceived the study. SZ, YC and CD wrote the paper. SZ, HL, and JX collected the
357 samples. SZ, TY and JX performed the measurement. All have contributed to review of the manuscript.

358
359 *Competing interests.* The authors declare that they have no conflict of interest.

360
361 *Acknowledgements.* This work is jointly supported by the National Key Research and Development Program of China
362 (2016YFA0601304), National Natural Science Foundation of China (41775145) and Fudan's Undergraduate Research
363 Opportunities Program (15100). We gratefully acknowledge the NOAA Air Resources Laboratory (ARL) for the provision of
364 the HYSPLIT model used in this publication and the National Climatic Data Center (NCDC) for the archived observed surface
365 meteorological data. The MODIS chlorophyll a data was downloaded from NASA OceanColor website
366 (<https://oceancolor.gsfc.nasa.gov/>). We are sincerely grateful to Huaniao Lighthouse maintained by Shanghai Maritime Safety



367 Administration for providing the long-term sampling site and fisherman Yueping Chen and his wife for sampling assistance at
368 Huaniao Island. We also thank all of the sailors onboard R/V *Dongfanghong II* for their logistical support during the cruise.
369 Shengqian Zhou sincerely acknowledge Bo Wang, Xiaofei Qin, Tianfeng Guo, Fanghui Wang and Yucheng Zhu for their
370 assistance with field and laboratory work.

371 References

- 372 Almeida, J., Schobesberger, S., Kurten, A., Ortega, I. K., Kupiainen-Maatta, O., Praplan, A. P., Adamov, A., Amorim, A.,
373 Bianchi, F., Breitenlechner, M., David, A., Dommen, J., Donahue, N. M., Downard, A., Dunne, E., Duplissy, J., Ehrhart, S.,
374 Flagan, R. C., Franchin, A., Guida, R., Hakala, J., Hansel, A., Heinritzi, M., Henschel, H., Jokinen, T., Junninen, H., Kajos,
375 M., Kangasluoma, J., Keskinen, H., Kupc, A., Kurten, T., Kvashin, A. N., Laaksonen, A., Lehtipalo, K., Leiminger, M., Leppa,
376 J., Loukonen, V., Makhmutov, V., Mathot, S., McGrath, M. J., Nieminen, T., Olenius, T., Onnela, A., Petaja, T., Riccobono, F.,
377 Riipinen, I., Rissanen, M., Rondo, L., Ruuskanen, T., Santos, F. D., Sarnela, N., Schallhart, S., Schnitzhofer, R., Seinfeld, J.
378 H., Simon, M., Sipila, M., Stozhkov, Y., Stratmann, F., Tome, A., Trostl, J., Tsagkogeorgas, G., Vaattovaara, P., Viisanen, Y.,
379 Virtanen, A., Vrtala, A., Wagner, P. E., Weingartner, E., Wex, H., Williamson, C., Wimmer, D., Ye, P., Yli-Juuti, T., Carslaw,
380 K. S., Kulmala, M., Curtius, J., Baltensperger, U., Worsnop, D. R., Vehkamäki, H., and Kirkby, J.: Molecular understanding
381 of sulphuric acid-amine particle nucleation in the atmosphere, *Nature*, 502, 359-363, <https://doi.org/10.1038/nature12663>,
382 2013.
- 383 Altieri, K. E., Hastings, M. G., Peters, A. J., Olenik, S., and Sigman, D. M.: Isotopic evidence for a marine ammonium source
384 in rainwater at Bermuda, *Global Biogeochem. Cy.*, 28, 1066-1080, <https://doi.org/10.1002/2014GB004809>, 2014.
- 385 Barnes, I., Hjorth, J., and Mihalopoulos, N.: Dimethyl sulfide and dimethyl sulfoxide and their oxidation in the atmosphere,
386 *Chem. Rev.*, 106, 940-975, <https://doi.org/10.1021/cr020529+>, 2006.
- 387 Bian, Q., Huang, X. H. H., and Yu, J. Z.: One-year observations of size distribution characteristics of major aerosol constituents
388 at a coastal receptor site in Hong Kong – Part 1: Inorganic ions and oxalate, *Atmos. Chem. Phys.*, 14, 9013-9027,
389 <https://doi.org/10.5194/acp-14-9013-2014>, 2014.
- 390 Calderón, S. M., Poor, N. D., and Campbell, S. W.: Estimation of the particle and gas scavenging contributions to wet
391 deposition of organic nitrogen, *Atmos. Environ.*, 41, 4281-4290, <https://doi.org/10.1016/j.atmosenv.2006.06.067>, 2007.
- 392 Chan, L. P., and Chan, C. K.: Role of the aerosol phase state in ammonia/amines exchange reactions, *Environ. Sci. Technol.*,
393 47, 5755-5762, <https://doi.org/10.1021/es4004685>, 2013.
- 394 Charlson, R. J., Lovelock, J. E., Andreaei, M. O., and Warren, S. G.: Oceanic phytoplankton, atmospheric sulphur, cloud albedo
395 and climate, *Nature*, 326, 655-661, <https://doi.org/10.1038/326655a0>, 1987.
- 396 Erupe, M. E., Viggiano, A. A., and Lee, S. H.: The effect of trimethylamine on atmospheric nucleation involving H₂SO₄, *Atmos.*
397 *Chem. Phys.*, 11, 4767-4775, <https://doi.org/10.5194/acp-11-4767-2011>, 2011.
- 398 Facchini, M. C., Decesari, S., Rinaldi, M., Carbone, C., Finessi, E., Mircea, M., Fuzzi, S., Moretti, F., Tagliavini, E., Ceburnis,
399 D., and O'Dowd, C. D.: Important source of marine secondary organic aerosol from biogenic amines, *Environ. Sci. Technol.*,
400 42, 9116-9121, <https://doi.org/10.1021/es8018385>, 2008.
- 401 Faloon, I.: Sulfur processing in the marine atmospheric boundary layer: A review and critical assessment of modeling
402 uncertainties, *Atmos. Environ.*, 43, 2841-2854, <https://doi.org/10.1016/j.atmosenv.2009.02.043>, 2009.
- 403 Ge, X., Wexler, A. S., and Clegg, S. L.: Atmospheric amines – Part II. Thermodynamic properties and gas/particle partitioning,
404 *Atmos. Environ.*, 45, 561-577, <https://doi.org/10.1016/j.atmosenv.2010.10.013>, 2011a.
- 405 Ge, X., Wexler, A. S., and Clegg, S. L.: Atmospheric amines – Part I. A review, *Atmos. Environ.*, 45, 524-546,
406 <https://doi.org/10.1016/j.atmosenv.2010.10.012>, 2011b.
- 407 Gibb, S. W., Mantoura, R. F. C., and Liss, P. S.: Ocean-atmosphere exchange and atmospheric speciation of ammonia and



- 408 methylamines in the region of the NW Arabian Sea, *Global Biogeochem. Cy.*, 13, 161-178, <https://doi.org/10.1029/98gb00743>,
409 1999.
- 410 Hemmilä, M., Hellén, H., Virkkula, A., Makkonen, U., Praplan, A. P., Kontkanen, J., Ahonen, L., Kulmala, M., and Hakola,
411 H.: Amines in boreal forest air at SMEAR II station in Finland, *Atmos. Chem. Phys.*, 18, 6367-6380,
412 <https://doi.org/10.5194/acp-18-6367-2018>, 2018.
- 413 Ho, K. F., Ho, S. S. H., Huang, R.-J., Liu, S. X., Cao, J.-J., Zhang, T., Chuang, H.-C., Chan, C. S., Hu, D., and Tian, L.:
414 Characteristics of water-soluble organic nitrogen in fine particulate matter in the continental area of China, *Atmos. Environ.*,
415 106, 252-261, <https://doi.org/10.1016/j.atmosenv.2015.02.010>, 2015.
- 416 Hu, Q., Yu, P., Zhu, Y., Li, K., Gao, H., and Yao, X.: Concentration, Size Distribution, and Formation of Trimethylammonium
417 and Dimethylammonium Ions in Atmospheric Particles over Marginal Seas of China, *J. Atmos. Sci.*, 72, 3487-3498,
418 <https://doi.org/10.1175/jas-d-14-0393.1>, 2015.
- 419 Hu, Q., Qu, K., Gao, H., Cui, Z., Gao, Y., and Yao, X.: Large increases in primary trimethylammonium and secondary
420 dimethylammonium in atmospheric particles associated with cyclonic eddies in the northwest Pacific Ocean, *J. Geophys. Res.-*
421 *Atmos.*, <https://doi.org/10.1029/2018jd028836>, 2018.
- 422 Huang, R. J., Li, W. B., Wang, Y. R., Wang, Q. Y., Jia, W. T., Ho, K. F., Cao, J. J., Wang, G. H., Chen, X., Ei Haddad, I., Zhuang,
423 Z. X., Wang, X. R., Prévôt, A. S. H., O'Dowd, C. D., and Hoffmann, T.: Determination of alkylamines in atmospheric aerosol
424 particles: a comparison of gas chromatography–mass spectrometry and ion chromatography approaches, *Atmos. Meas. Tech.*,
425 7, 2027-2035, <https://doi.org/10.5194/amt-7-2027-2014>, 2014.
- 426 Huang, X., Deng, C., Zhuang, G., Lin, J., and Xiao, M.: Quantitative analysis of aliphatic amines in urban aerosols based on
427 online derivatization and high performance liquid chromatography, *Environ. Sci.-Proc. Imp.*, 18, 796-801,
428 <https://doi.org/10.1039/c6em00197a>, 2016.
- 429 Huang, Y., Chen, H., Wang, L., Yang, X., and Chen, J.: Single particle analysis of amines in ambient aerosol in Shanghai,
430 *Environ. Chem.*, 9, 202, <https://doi.org/10.1071/en11145>, 2012.
- 431 Kupiainen, O., Ortega, I. K., Kurten, T., and Vehkamäki, H.: Amine substitution into sulfuric acid - ammonia clusters, *Atmos.*
432 *Chem. Phys.*, 12, 3591-3599, <https://doi.org/10.5194/acp-12-3591-2012>, 2012.
- 433 Kurten, A., Jokinen, T., Simon, M., Sipilä, M., Sarnela, N., Junninen, H., Adamov, A., Almeida, J., Amorim, A., Bianchi, F.,
434 Breitenlechner, M., Dommen, J., Donahue, N. M., Duplissy, J., Ehrhart, S., Flagan, R. C., Franchin, A., Hakala, J., Hansel, A.,
435 Heinritzi, M., Hutterli, M., Kangasluoma, J., Kirkby, J., Laaksonen, A., Lehtipalo, K., Leiminger, M., Makhmutov, V., Mathot,
436 S., Onnela, A., Petaja, T., Praplan, A. P., Riccobono, F., Rissanen, M. P., Rondo, L., Schobesberger, S., Seinfeld, J. H., Steiner,
437 G., Tome, A., Trostl, J., Winkler, P. M., Williamson, C., Wimmer, D., Ye, P., Baltensperger, U., Carslaw, K. S., Kulmala, M.,
438 Worsnop, D. R., and Curtius, J.: Neutral molecular cluster formation of sulfuric acid-dimethylamine observed in real time
439 under atmospheric conditions, *P. Natl. Acad. Sci. USA*, 111, 15019-15024, <https://doi.org/10.1073/pnas.1404853111>, 2014.
- 440 Kürten, A., Bergen, A., Heinritzi, M., Leiminger, M., Lorenz, V., Piel, F., Simon, M., Sitals, R., Wagner, A. C., and Curtius, J.:
441 Observation of new particle formation and measurement of sulfuric acid, ammonia, amines and highly oxidized organic
442 molecules at a rural site in central Germany, *Atmos. Chem. Phys.*, 16, 12793-12813, [https://doi.org/10.5194/acp-16-12793-](https://doi.org/10.5194/acp-16-12793-2016)
443 2016, 2016.
- 444 Kurten, T., Loukonen, V., Vehkamäki, H., and Kulmala, M.: Amines are likely to enhance neutral and ion-induced sulfuric
445 acid-water nucleation in the atmosphere more effectively than ammonia, *Atmos. Chem. Phys.*, 8, 4095-4103,
446 <https://doi.org/10.5194/acp-8-4095-2008>, 2008.
- 447 Liu, F., Bi, X., Zhang, G., Peng, L., Lian, X., Lu, H., Fu, Y., Wang, X., Peng, P. a., and Sheng, G.: Concentration, size
448 distribution and dry deposition of amines in atmospheric particles of urban Guangzhou, China, *Atmos. Environ.*, 171, 279-288,
449 <https://doi.org/10.1016/j.atmosenv.2017.10.016>, 2017.
- 450 Liu, F., Bi, X., Zhang, G., Lian, X., Fu, Y., Yang, Y., Lin, Q., Jiang, F., Wang, X., Peng, P. a., and Sheng, G.: Gas-to-particle



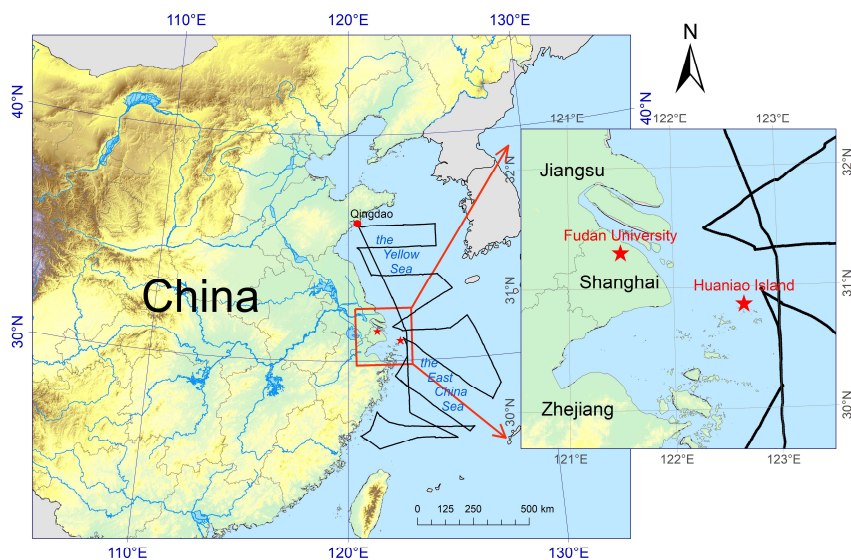
- 451 partitioning of atmospheric amines observed at a mountain site in southern China, *Atmos. Environ.*, 195, 1-11,
452 <https://doi.org/10.1016/j.atmosenv.2018.09.038>, 2018a.
- 453 Liu, X.-H., Zhang, Y., Cheng, S.-H., Xing, J., Zhang, Q., Streets, D. G., Jang, C., Wang, W.-X., and Hao, J.-M.: Understanding
454 of regional air pollution over China using CMAQ, part I performance evaluation and seasonal variation, *Atmos. Environ.*, 44,
455 2415-2426, <https://doi.org/10.1016/j.atmosenv.2010.03.035>, 2010.
- 456 Liu, X., Li, J., Qu, Y., Han, T., Hou, L., Gu, J., Chen, C., Yang, Y., Liu, X., and Yang, T.: Formation and evolution mechanism
457 of regional haze: a case study in the megacity Beijing, China, *Atmos. Chem. Phys.*, 13, 4501-4514, <https://doi.org/10.5194/acp-13-4501-2013>, 2013.
- 459 Liu, Y., Han, C., Liu, C., Ma, J., Ma, Q., and He, H.: Differences in the reactivity of ammonium salts with methylamine, *Atmos.*
460 *Chem. Phys.*, 12, 4855-4865, <https://doi.org/10.5194/acp-12-4855-2012>, 2012.
- 461 Liu, Y., Fan, Q., Chen, X., Zhao, J., Ling, Z., Hong, Y., Li, W., Chen, X., Wang, M., and Wei, X.: Modeling the impact of
462 chlorine emissions from coal combustion and prescribed waste incineration on tropospheric ozone formation in China, *Atmos.*
463 *Chem. Phys.*, 18, 2709-2724, <https://doi.org/10.5194/acp-18-2709-2018>, 2018b.
- 464 Logan, J. A.: Tropospheric ozone: Seasonal behavior, trends, and anthropogenic influence, *J. Geophys. Res.-Atmos.*, 90,
465 10463-10482, <https://doi.org/10.1029/JD090iD06p10463>, 1985.
- 466 Loukonen, V., Kurtén, T., Ortega, I. K., Vehkamäki, H., Pádua, A. A. H., Sellegri, K., and Kulmala, M.: Enhancing effect of
467 dimethylamine in sulfuric acid nucleation in the presence of water – a computational study, *Atmos. Chem. Phys.*, 10, 4961-
468 4974, <https://doi.org/10.5194/acp-10-4961-2010>, 2010.
- 469 Müller, C., Iinuma, Y., Karstensen, J., van Pinxteren, D., Lehmann, S., Gnauk, T., and Herrmann, H.: Seasonal variation of
470 aliphatic amines in marine sub-micrometer particles at the Cape Verde islands, *Atmos. Chem. Phys.*, 9, 9587-9597,
471 <https://doi.org/10.5194/acp-9-9587-2009>, 2009.
- 472 Murphy, S. M., Sorooshian, A., Kroll, J. H., Ng, N. L., Chhabra, P., Tong, C., Surratt, J. D., Knipping, E., Flagan, R. C., and
473 Seinfeld, J. H.: Secondary aerosol formation from atmospheric reactions of aliphatic amines, *Atmos. Chem. Phys.*, 7, 2313-
474 2337, <https://doi.org/10.5194/acp-7-2313-2007>, 2007.
- 475 Nielsen, C. J., Herrmann, H., and Weller, C.: Atmospheric chemistry and environmental impact of the use of amines in carbon
476 capture and storage (CCS), *Chem. Soc. Rev.*, 41, 6684-6704, <https://doi.org/10.1039/c2cs35059a>, 2012.
- 477 Olenius, T., Halonen, R., Kurtén, T., Henschel, H., Kupiainen-Määttä, O., Ortega, I. K., Jen, C. N., Vehkamäki, H., and Riipinen,
478 I.: New particle formation from sulfuric acid and amines: Comparison of monomethylamine, dimethylamine, and
479 trimethylamine, *J. Geophys. Res.-Atmos.*, 122, 7103-7118, <https://doi.org/10.1002/2017jd026501>, 2017.
- 480 Paasonen, P., Olenius, T., Kupiainen, O., Kurten, T., Petaja, T., Birmili, W., Hamed, A., Hu, M., Huey, L. G., Plass-Duelmer,
481 C., Smith, J. N., Wiedensohler, A., Loukonen, V., McGrath, M. J., Ortega, I. K., Laaksonen, A., Vehkamäki, H., Kerminen, V.
482 M., and Kulmala, M.: On the formation of sulphuric acid - amine clusters in varying atmospheric conditions and its influence
483 on atmospheric new particle formation, *Atmos. Chem. Phys.*, 12, 9113-9133, <https://doi.org/10.5194/acp-12-9113-2012>, 2012.
- 484 Pankow, J. F.: Phase considerations in the gas/particle partitioning of organic amines in the atmosphere, *Atmos. Environ.*, 122,
485 448-453, <https://doi.org/10.1016/j.atmosenv.2015.09.056>, 2015.
- 486 Paulot, F., Jacob, D. J., Johnson, M. T., Bell, T. G., Baker, A. R., Keene, W. C., Lima, I. D., Doney, S. C., and Stock, C. A.:
487 Global oceanic emission of ammonia: Constraints from seawater and atmospheric observations, *Global Biogeochem. Cy.*, 29,
488 1165-1178, <https://doi.org/10.1002/2015gb005106>, 2015.
- 489 Perrone, M. G., Zhou, J., Malandrino, M., Sangiorgi, G., Rizzi, C., Ferrero, L., Dommen, J., and Bolzacchini, E.: PM chemical
490 composition and oxidative potential of the soluble fraction of particles at two sites in the urban area of Milan, Northern Italy,
491 *Atmos. Environ.*, 128, 104-113, <https://doi.org/10.1016/j.atmosenv.2015.12.040>, 2016.
- 492 Rehbein, P. J., Jeong, C. H., McGuire, M. L., Yao, X., Corbin, J. C., and Evans, G. J.: Cloud and fog processing enhanced gas-
493 to-particle partitioning of trimethylamine, *Environ. Sci. Technol.*, 45, 4346-4352, <https://doi.org/10.1021/es1042113>, 2011.



- 494 Saltzman, E., Savoie, D., Prospero, J., and Zika, R.: Atmospheric methanesulfonic acid and non - sea - salt sulfate at Fanning
495 and American Samoa, *Geophys. Res. Lett.*, 12, 437-440, <https://doi.org/10.1029/GL012i007p00437>, 1985.
- 496 Shen, W., Ren, L., Zhao, Y., Zhou, L., Dai, L., Ge, X., Kong, S., Yan, Q., Xu, H., Jiang, Y., He, J., Chen, M., and Yu, H.: C1-
497 C2 alkyl aminiums in urban aerosols: Insights from ambient and fuel combustion emission measurements in the Yangtze River
498 Delta region of China, *Environ. Pollut.*, 230, 12-21, <https://doi.org/10.1016/j.envpol.2017.06.034>, 2017.
- 499 Smith, J. N., Barsanti, K. C., Friedli, H. R., Ehn, M., Kulmala, M., Collins, D. R., Scheckman, J. H., Williams, B. J., and
500 McMurry, P. H.: Observations of aminium salts in atmospheric nanoparticles and possible climatic implications, *P. Natl. Acad.*
501 *Sci. USA*, 107, 6634-6639, <https://doi.org/10.1073/pnas.0912127107>, 2010.
- 502 Sorooshian, A., Padró, L. T., Nenes, A., Feingold, G., McComiskey, A., Hersey, S. P., Gates, H., Jonsson, H. H., Miller, S. D.,
503 Stephens, G. L., Flagan, R. C., and Seinfeld, J. H.: On the link between ocean biota emissions, aerosol, and maritime clouds:
504 Airborne, ground, and satellite measurements off the coast of California, *Global Biogeochem. Cy.*, 23, n/a-n/a,
505 <https://doi.org/10.1029/2009gb003464>, 2009.
- 506 Souza, S.: Low molecular weight carboxylic acids in an urban atmosphere: Winter measurements in São Paulo City, Brazil,
507 *Atmos. Environ.*, 33, 2563-2574, [https://doi.org/10.1016/s1352-2310\(98\)00383-5](https://doi.org/10.1016/s1352-2310(98)00383-5), 1999.
- 508 Tang, X., Price, D., Praske, E., Vu, D. N., Purvis-Roberts, K., Silva, P. J., Cocker Iii, D. R., and Asa-Awuku, A.: Cloud
509 condensation nuclei (CCN) activity of aliphatic amine secondary aerosol, *Atmos. Chem. Phys.*, 14, 5959-5967,
510 <https://doi.org/10.5194/acp-14-5959-2014>, 2014.
- 511 Tao, Y., Ye, X., Jiang, S., Yang, X., Chen, J., Xie, Y., and Wang, R.: Effects of amines on particle growth observed in new
512 particle formation events, *J. Geophys. Res.-Atmos.*, 121, 324-335, <https://doi.org/10.1002/2015jd024245>, 2016.
- 513 Tao, Y., and Murphy, J. G.: Evidence for the importance of semi-volatile organic ammonium salts in ambient particulate matter,
514 *Environ. Sci. Technol.*, 53, 108-116, <https://doi.org/10.1021/acs.est.8b03800>, 2018.
- 515 Thompson, A. M.: The oxidizing capacity of the Earth's atmosphere: Probable past and future changes, *Science*, 256, 1157-
516 1165, <https://doi.org/10.1126/science.256.5060.1157>, 1992.
- 517 Tian, H. Z., Zhu, C. Y., Gao, J. J., Cheng, K., Hao, J. M., Wang, K., Hua, S. B., Wang, Y., and Zhou, J. R.: Quantitative
518 assessment of atmospheric emissions of toxic heavy metals from anthropogenic sources in China: historical trend, spatial
519 distribution, uncertainties, and control policies, *Atmos. Chem. Phys.*, 15, 10127-10147, [https://doi.org/10.5194/acp-15-10127-](https://doi.org/10.5194/acp-15-10127-2015)
520 2015, 2015.
- 521 Tsai, Y. I., Sopajaree, K., Chotruksa, A., Wu, H.-C., and Kuo, S.-C.: Source indicators of biomass burning associated with
522 inorganic salts and carboxylates in dry season ambient aerosol in Chiang Mai Basin, Thailand, *Atmos. Environ.*, 78, 93-104,
523 <https://doi.org/10.1016/j.atmosenv.2012.09.040>, 2013.
- 524 Uno, I., Osada, K., Yumimoto, K., Wang, Z., Itahashi, S., Pan, X., Hara, Y., Kanaya, Y., Yamamoto, S., and Fairlie, T. D.:
525 Seasonal variation of fine- and coarse-mode nitrates and related aerosols over East Asia: synergetic observations and chemical
526 transport model analysis, *Atmos. Chem. Phys.*, 17, 14181-14197, <https://doi.org/10.5194/acp-17-14181-2017>, 2017.
- 527 VandenBoer, T. C., Petroff, A., Markovic, M. Z., and Murphy, J. G.: Size distribution of alkyl amines in continental particulate
528 matter and their online detection in the gas and particle phase, *Atmos. Chem. Phys.*, 11, 4319-4332,
529 <https://doi.org/10.5194/acp-11-4319-2011>, 2011.
- 530 VandenBoer, T. C., Markovic, M. Z., Petroff, A., Czar, M. F., Borduas, N., and Murphy, J. G.: Ion chromatographic separation
531 and quantitation of alkyl methylamines and ethylamines in atmospheric gas and particulate matter using preconcentration and
532 suppressed conductivity detection, *J. Chromatogr. A*, 1252, 74-83, <https://doi.org/10.1016/j.chroma.2012.06.062>, 2012.
- 533 Violaki, K., and Mihalopoulos, N.: Water-soluble organic nitrogen (WSON) in size-segregated atmospheric particles over the
534 Eastern Mediterranean, *Atmos. Environ.*, 44, 4339-4345, <https://doi.org/10.1016/j.atmosenv.2010.07.056>, 2010.
- 535 Wang, B., Chen, Y., Zhou, S., Li, H., Wang, F., and Yang, T.: The influence of terrestrial transport on visibility and aerosol
536 properties over the coastal East China Sea, *Sci. Total. Environ.*, 649, 652-660, <https://doi.org/10.1016/j.scitotenv.2018.08.312>,

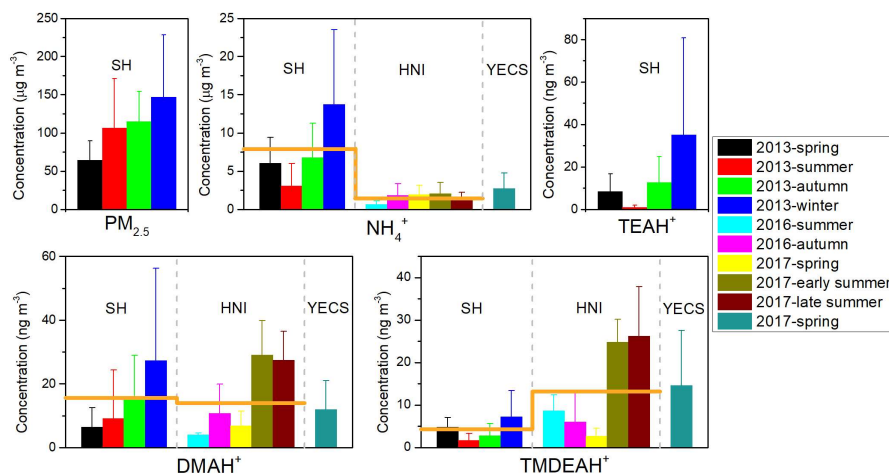


- 537 2018.
- 538 Wang, F., Chen, Y., Meng, X., Fu, J., and Wang, B.: The contribution of anthropogenic sources to the aerosols over East China
539 Sea, *Atmos. Environ.*, 127, 22-33, <https://doi.org/10.1016/j.atmosenv.2015.12.002>, 2016.
- 540 Wang, L., Khalizov, A. F., Zheng, J., Xu, W., Ma, Y., Lal, V., and Zhang, R.: Atmospheric nanoparticles formed from
541 heterogeneous reactions of organics, *Nat. Geosci.*, 3, 238-242, <https://doi.org/10.1038/ngeo778>, 2010a.
- 542 Wang, L., Lal, V., Khalizov, A. F., and Zhang, R.: Heterogeneous chemistry of alkylamines with sulfuric acid: implications for
543 atmospheric formation of alkylammonium sulfates, *Environ. Sci. Technol.*, 44, 2461-2465, <https://doi.org/10.1021/es9036868>,
544 2010b.
- 545 Xie, H., Feng, L., Hu, Q., Zhu, Y., Gao, H., Gao, Y., and Yao, X.: Concentration and size distribution of water-extracted
546 dimethylammonium and trimethylammonium in atmospheric particles during nine campaigns - Implications for sources, phase
547 states and formation pathways, *Sci. Total. Environ.*, 631-632, 130-141, <https://doi.org/10.1016/j.scitotenv.2018.02.303>, 2018.
- 548 Yang, G.-P., Zhang, H.-H., Su, L.-P., and Zhou, L.-M.: Biogenic emission of dimethylsulfide (DMS) from the North Yellow
549 Sea, China and its contribution to sulfate in aerosol during summer, *Atmos. Environ.*, 43, 2196-2203,
550 <https://doi.org/10.1016/j.atmosenv.2009.01.011>, 2009.
- 551 Yang, G.-P., Zhang, S.-H., Zhang, H.-H., Yang, J., and Liu, C.-Y.: Distribution of biogenic sulfur in the Bohai Sea and northern
552 Yellow Sea and its contribution to atmospheric sulfate aerosol in the late fall, *Mar. Chem.*, 169, 23-32,
553 <https://doi.org/10.1016/j.marchem.2014.12.008>, 2015.
- 554 Yao, L., Wang, M.-Y., Wang, X.-K., Liu, Y.-J., Chen, H.-F., Zheng, J., Nie, W., Ding, A.-J., Geng, F.-H., Wang, D.-F., Chen,
555 J.-M., Worsnop, D. R., and Wang, L.: Detection of atmospheric gaseous amines and amides by a high-resolution time-of-flight
556 chemical ionization mass spectrometer with protonated ethanol reagent ions, *Atmos. Chem. Phys.*, 16, 14527-14543,
557 <https://doi.org/10.5194/acp-16-14527-2016>, 2016.
- 558 Yao, L., Garmash, O., Bianchi, F., Zheng, J., Yan, C., Kontkanen, J., Junninen, H., Mazon, S. B., Ehn, M., Paasonen, P., Sipila,
559 M., Wang, M., Wang, X., Xiao, S., Chen, H., Lu, Y., Zhang, B., Wang, D., Fu, Q., Geng, F., Li, L., Wang, H., Qiao, L., Yang,
560 X., Chen, J., Kerminen, V. M., Petaja, T., Worsnop, D. R., Kulmala, M., and Wang, L.: Atmospheric new particle formation
561 from sulfuric acid and amines in a Chinese megacity, *Science*, 361, 278-281, <https://doi.org/10.1126/science.aao4839>, 2018.
- 562 Yu, F., and Luo, G.: Modeling of gaseous methylamines in the global atmosphere: impacts of oxidation and aerosol uptake,
563 *Atmos. Chem. Phys.*, 14, 12455-12464, <https://doi.org/10.5194/acp-14-12455-2014>, 2014.
- 564 Yu, H., McGraw, R., and Lee, S.-H.: Effects of amines on formation of sub-3 nm particles and their subsequent growth,
565 *Geophys. Res. Lett.*, 39, n/a-n/a, <https://doi.org/10.1029/2011gl050099>, 2012.
- 566 Yu, P., Hu, Q., Li, K., Zhu, Y., Liu, X., Gao, H., and Yao, X.: Characteristics of dimethylammonium and trimethylammonium in
567 atmospheric particles ranging from supermicron to nanometer sizes over eutrophic marginal seas of China and oligotrophic
568 open oceans, *Sci. Total. Environ.*, 572, 813-824, <https://doi.org/10.1016/j.scitotenv.2016.07.114>, 2016.
- 569 Yuan, H., Wang, Y., and Zhuang, G.: MSA in Beijing aerosol, *Chinese Sci. Bull.*, 49, 1020, 10.1360/03wb0186, 2004.
- 570 Zhang, G., Bi, X., Chan, L. Y., Li, L., Wang, X., Feng, J., Sheng, G., Fu, J., Li, M., and Zhou, Z.: Enhanced trimethylamine-
571 containing particles during fog events detected by single particle aerosol mass spectrometry in urban Guangzhou, China, *Atmos.*
572 *Environ.*, 55, 121-126, <https://doi.org/10.1016/j.atmosenv.2012.03.038>, 2012.
- 573 Zheng, J., Ma, Y., Chen, M., Zhang, Q., Wang, L., Khalizov, A. F., Yao, L., Wang, Z., Wang, X., and Chen, L.: Measurement
574 of atmospheric amines and ammonia using the high resolution time-of-flight chemical ionization mass spectrometry, *Atmos.*
575 *Environ.*, 102, 249-259, <https://doi.org/10.1016/j.atmosenv.2014.12.002>, 2015.
- 576 Zhou, S., Lin, J., Qin, X., Chen, Y., and Deng, C.: Determination of atmospheric alkylamines by ion chromatography using
577 18-crown-6 as mobile phase additive, *J Chromatogr. A*, 1563, 154-161, <https://doi.org/10.1016/j.chroma.2018.05.074>, 2018.
- 578
- 579



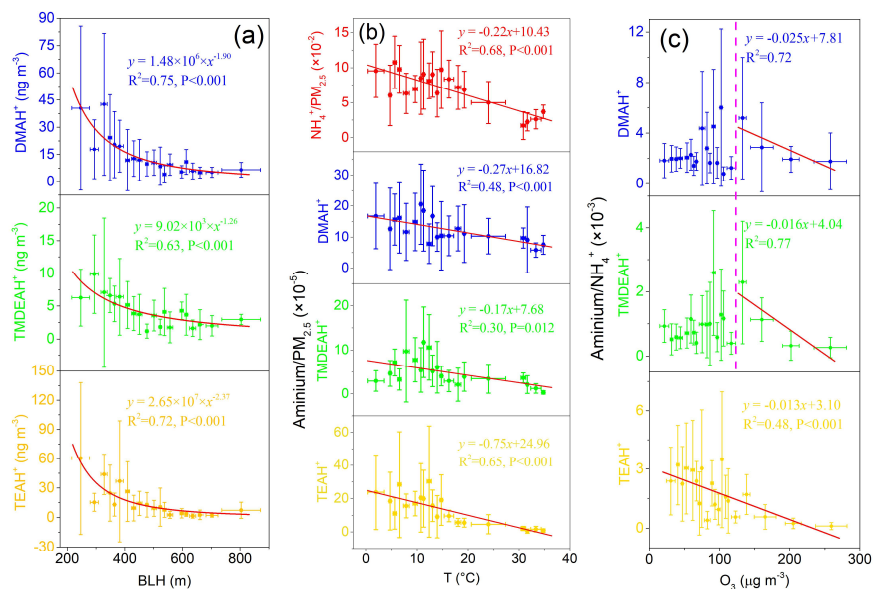
580

581 **Figure 1.** Map of sampling sites and area. The red stars represent the locations of Shanghai (Fudan University) and the
 582 Huaniao Island, and the black line in the marginal seas represents the cruise track in the spring of 2017.



583

584 **Figure 2.** The mass concentrations of $PM_{2.5}$, fine-particle NH_4^+ and three aminiums ($TEAH^+$, $DMAH^+$ and $TMDEAH^+$) in different
 585 campaigns in Shanghai (SH), Huaniao Island (HNI) and the Yellow and East China seas (YECS). The columns and error bars represent
 586 average concentrations and standard deviations, respectively. The orange horizontal lines represent the annual average concentrations of
 587 aminiums in SH and HNI.

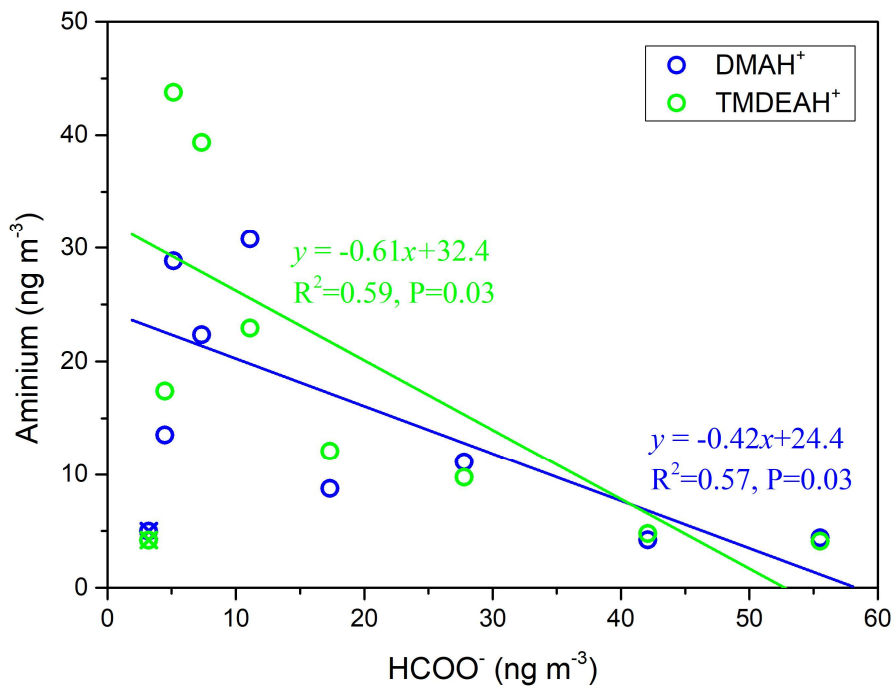


588

589

590

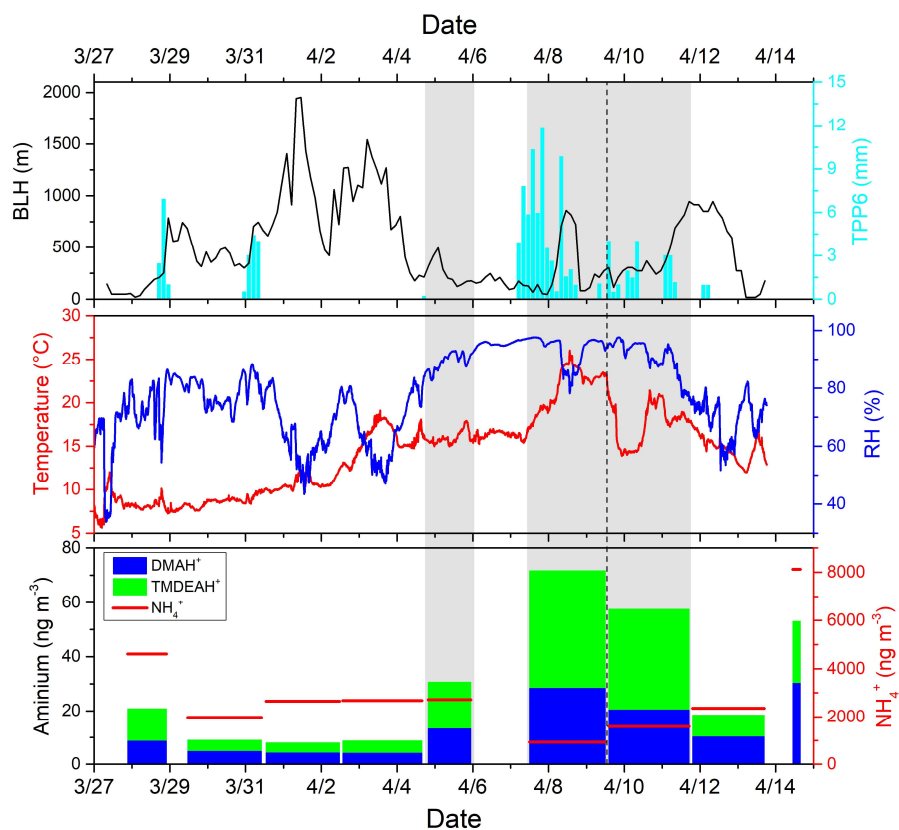
Figure 3. (a) Relationships between concentrations of aminiums and boundary layer height (BLH). (b) Relationships between mass ratios of aminiums and NH₄⁺ to PM_{2.5} and temperature. (c) Relationships between mass ratios of aminiums to NH₄⁺ and O₃ concentrations.



591

592

Figure 4. Correlations between concentrations of aminiums and HCOO⁻ over the Yellow and East China seas (YECS) in the spring of 2017.

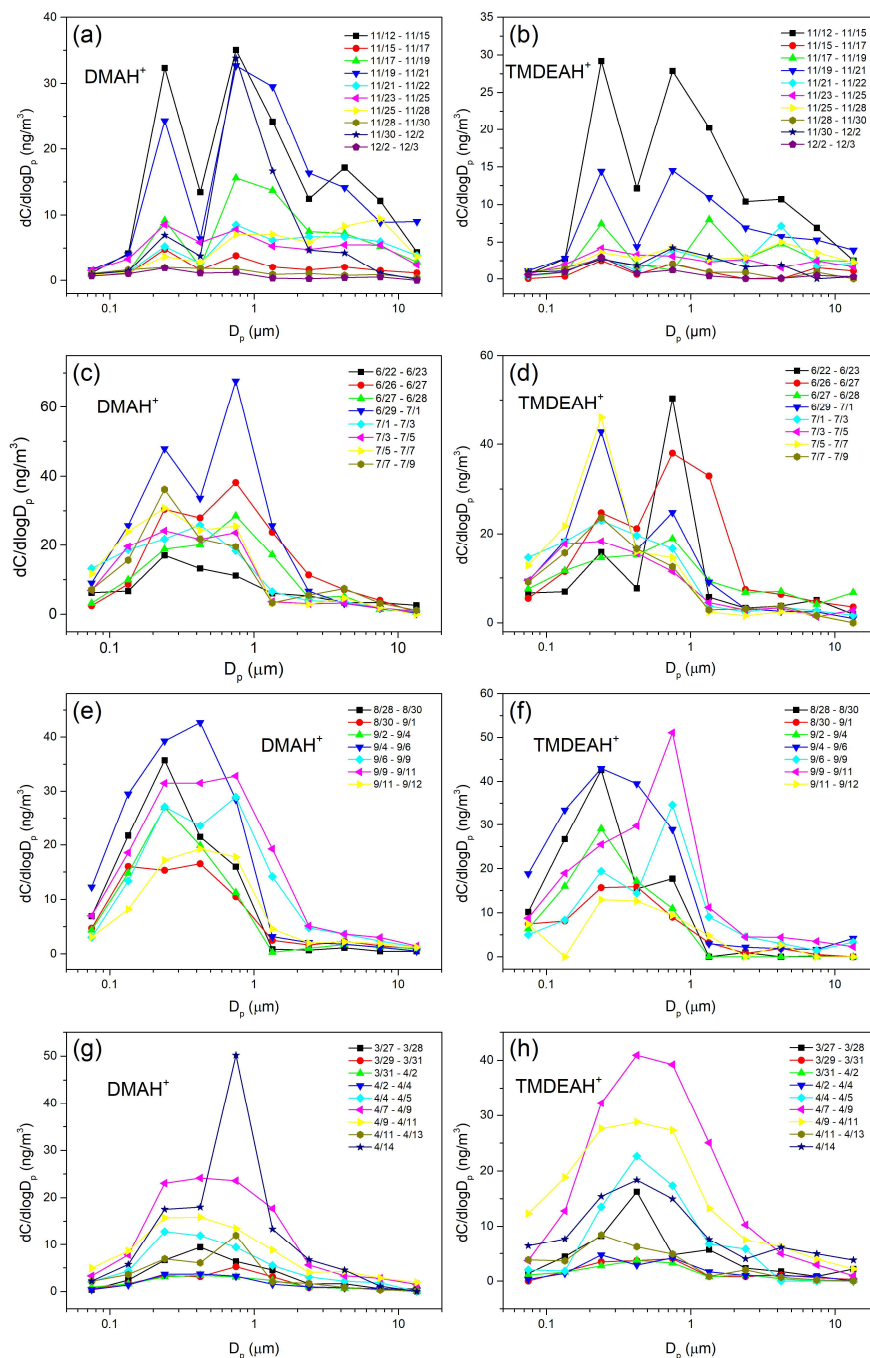


593

594

595

Figure 5. Time series of meteorological parameters and the concentrations of aminiums and NH_4^+ during the cruise of 2017. The time range spanned by the column of each aminium concentration corresponds to the sampling time.

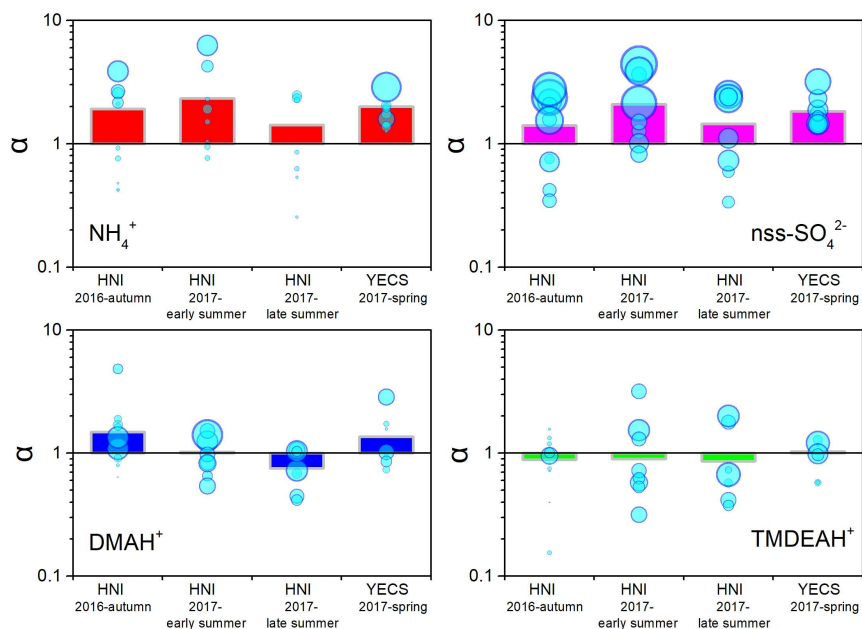


596

597

598

Figure 6. Size distributions of aminiums during different campaigns. (a-b): in the autumn of 2016 at Huaniao Island, (c-d): in early summer of 2017 at Huaniao Island, (e-f): in late summer of 2017 at Huaniao Island, (g-h): in 2017 spring cruise over the Yellow and East China seas.

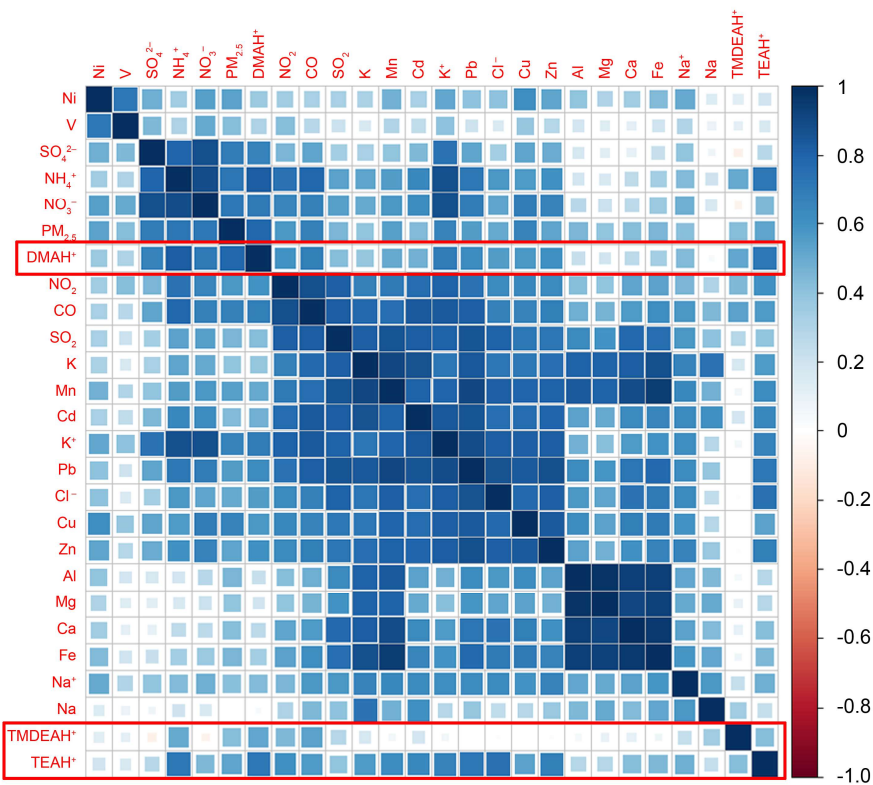


599

600

601

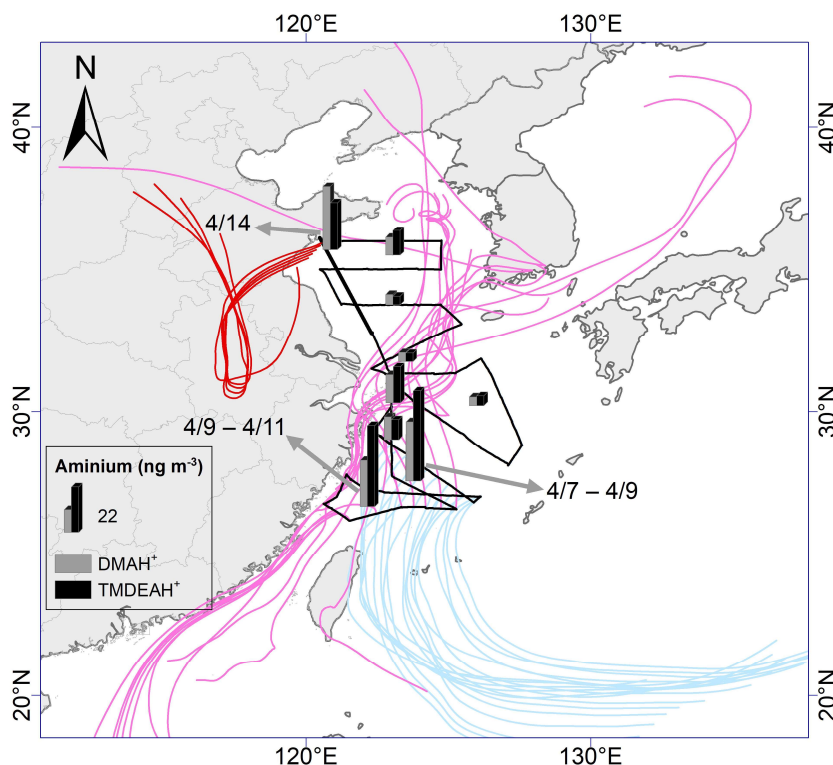
Figure 7. The α values of NH_4^+ , nss-SO_4^{2-} and aminiums in different campaigns. The diameter of the circle is proportional to the concentration and the column is the average value of α for each campaign. It should be noted that the bottom of column is the line of $\alpha=1$.



602

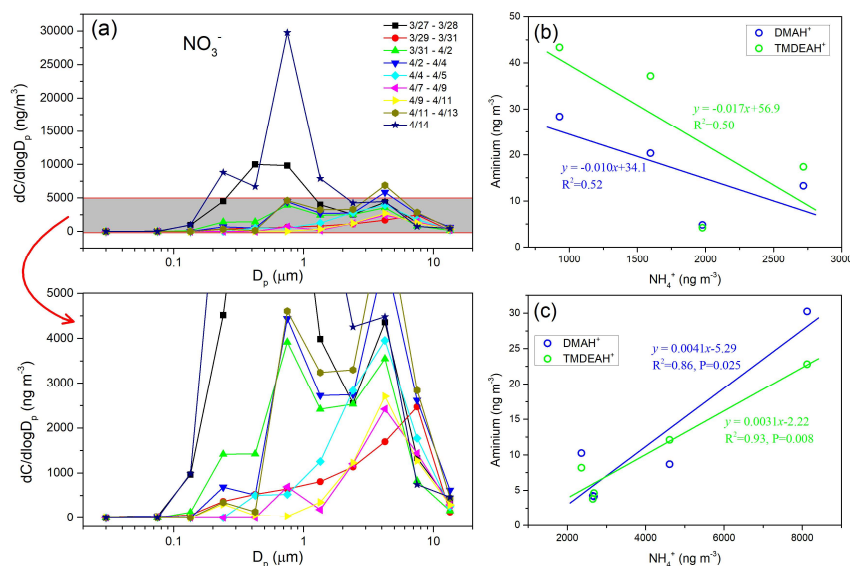
603

Figure 8. Correlation coefficient matrix among the concentrations of $\text{PM}_{2.5}$ components and gaseous pollutants over Shanghai in 2013.



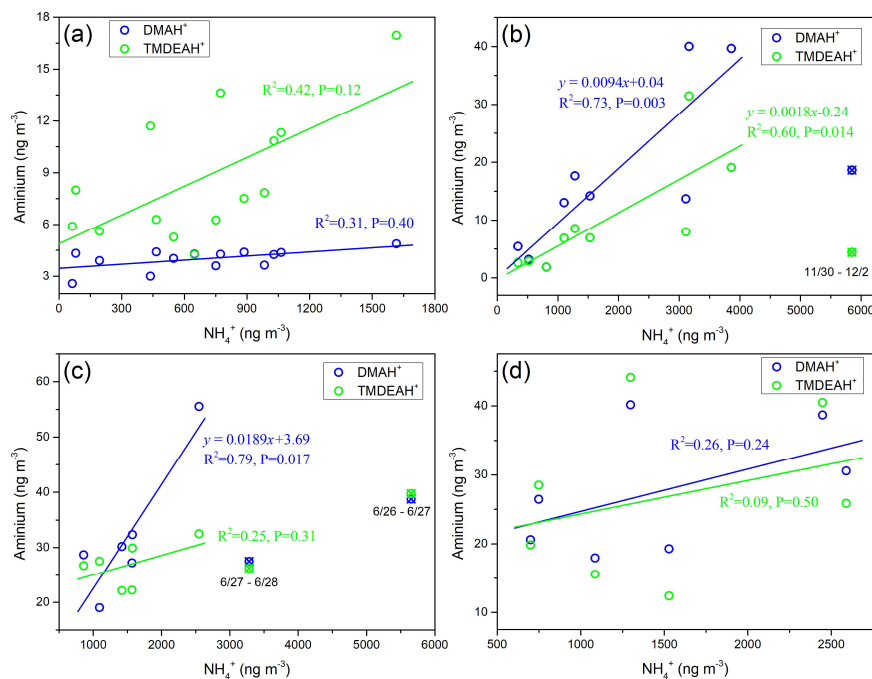
604

605 **Figure 9.** The spatial distribution of aminiums over the YECS in the spring of 2017. The ocean color represents the concentration of
 606 chlorophyll a obtained from Kriging interpolation from the observed concentrations. The light blue, pink and red lines represent 72-hour
 607 backward trajectories corresponding to sample sets collected on 7–9 Apr., 9–11 Apr. and 14 Apr., respectively.



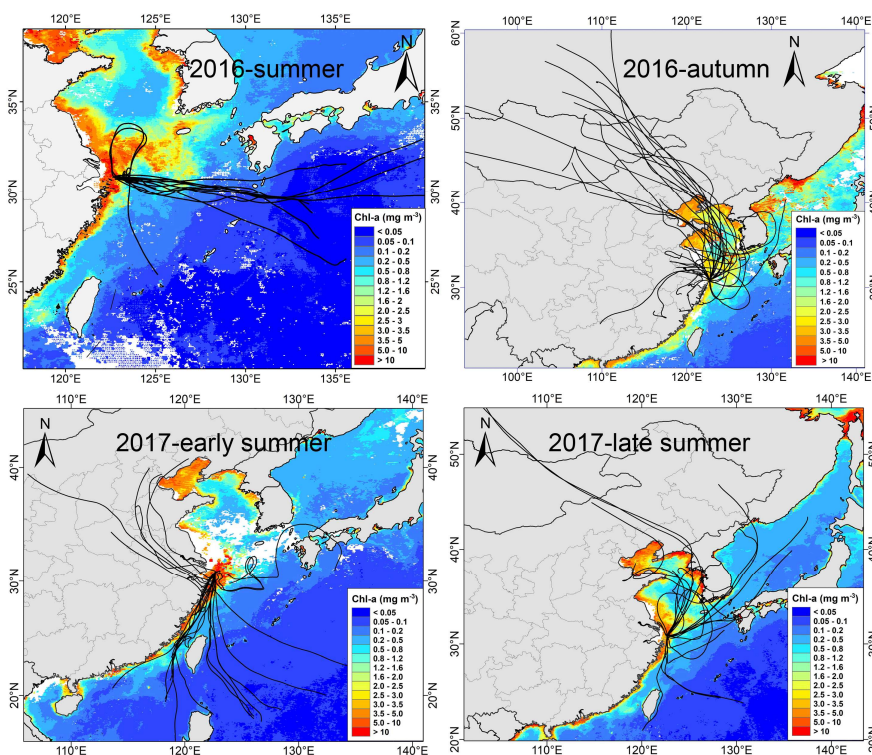
608

609 **Figure 10.** (a) Size distributions of NO_3^- over the YECS in the spring of 2017. (b) Correlations between concentrations of aminiums and
 610 NH_4^+ for the samples mainly influenced by marine air masses. (c) Correlations between concentrations of aminiums and NH_4^+ for the samples
 611 predominantly influenced by terrestrial transport.



612

613 **Figure 11.** Correlations between ammoniums and NH_4^+ concentrations over Huaniao Island for each campaign. (a): in the summer of 2016,
614 (b): in the autumn of 2016, (c): in early summer of 2017, (d): in late summer of 2017.

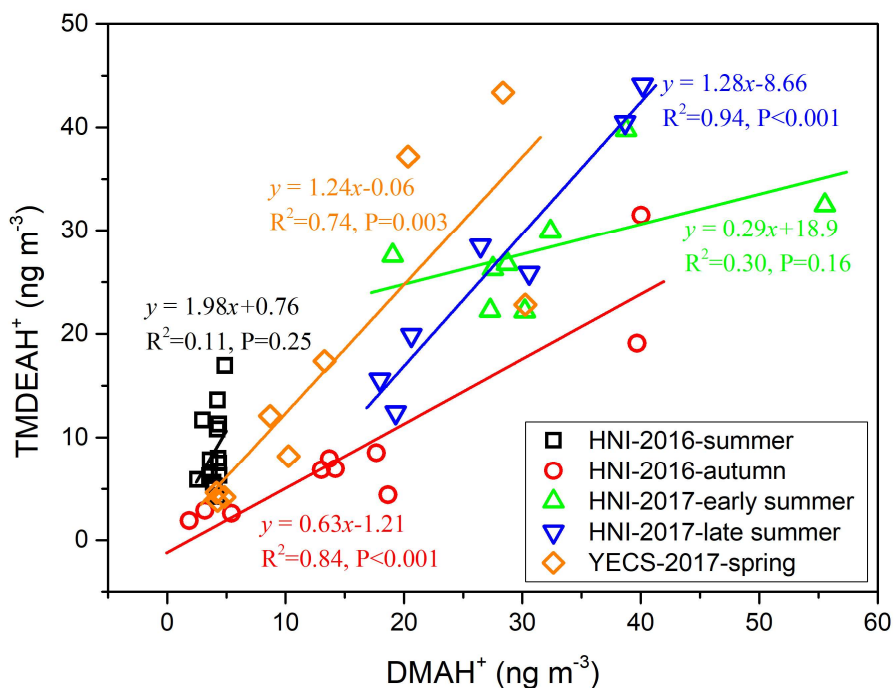


615

616 **Figure 12.** The 72-hour backward trajectories starting from Huaniao Island and the average chlorophyll a concentration retrieved and
617 combined from aqua- and terra-MODIS during the sampling period. Each sample during the summer of 2016 corresponds to one trajectory

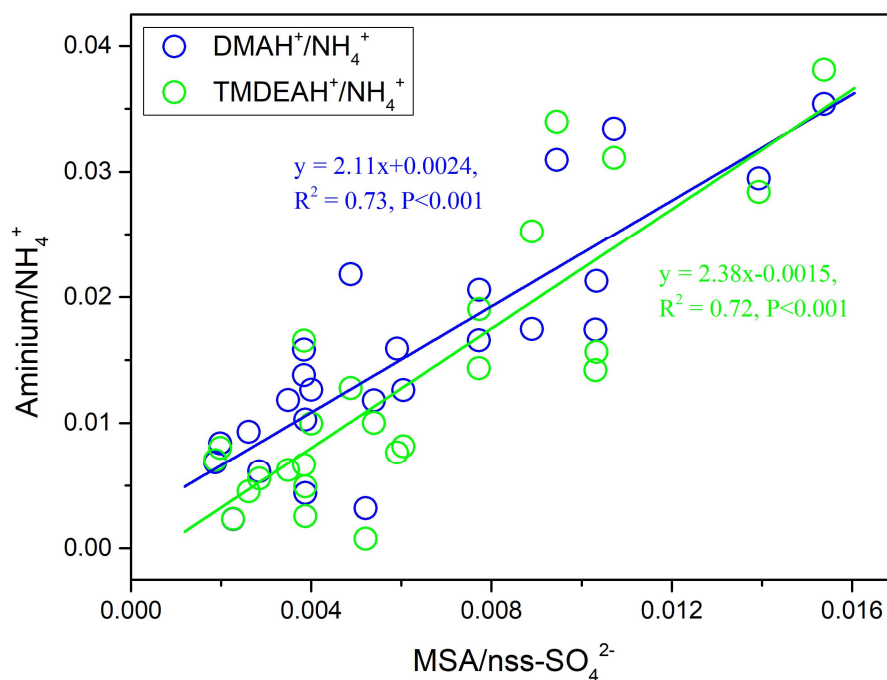


618 with a starting time in the middle of sampling period. Each sample set during the autumn of 2016 and the summer of 2017 corresponds to 3
619 trajectories and the starting times are taken at equal intervals in the sampling period.



620

621 **Figure 13.** Correlations between DMAH⁺ and TMDEAH⁺ for each campaign over Huaniao Island and the YECS.



622

623 **Figure 14.** Correlations between ammonium/NH₄⁺ and MSA/nss-SO₄²⁻ over Huaniao Island during the autumn in 2016 and the summer in
624 2017.

625

626 **Table 1.** Summary of sampling information in different campaigns.

Sampling site	Sampler	Sampling period	Number of samples or sample sets
		25 Mar. 2013–26 Apr. 2013 (spring)	29
Fudan University, Shanghai	Medium-flow PM _{2.5} sampler	16 Jul. 2013–17 Aug. 2013 (summer)	26
		30 Oct. 2013–30 Nov. 2013 (autumn)	29
		1 Dec. 2013–23 Jan. 2014 (winter)	47
Huaniao Island	Medium-flow PM _{2.5} sampler	4 Aug. 2016–18 Aug. 2016 (summer)	14
		12 Nov. 2016–3 Dec. 2016 (autumn)	9
Huaniao Island	MOUDI	11 Mar. 2017–19 Mar. 2017 (spring)	4
		22 Jun. 2017–9 Jul. 2017 (early summer)	8
		27 Aug. 2017–12 Sep. 2017 (late summer)	7
the Yellow Sea and the East China Sea	MOUDI	27 Mar. 2017–14 Apr. 2017 (spring)	9

627

628



Table 2. The mass concentrations of NH_4^+ and ammoniums over Shanghai, Huanisao Island and the YECs compared to other sites reported in literatures. The values below the detection limits are indicated by < DL.

No.	Site	Site type	Sampling period	Particle size	NH_4^+ ($\mu\text{g m}^{-3}$)	Ammonium (ng m^{-3})					Reference
						MMAH ⁺	DMAH ⁺	TMDEAH ⁺	MEA ⁺	TEAH ⁺	
1	Shanghai	urban	Spring (Mar–Apr. 2013)	$\text{PM}_{2.5}$	6.0 ± 3.4	6.4 ± 6.1	4.8 ± 2.3	8.4 ± 8.4		this study	
2			Summer (Jul–Aug. 2013)	$\text{PM}_{2.5}$	3.1 ± 2.9	9.1 ± 15.2	1.7 ± 1.6	0.9 ± 1.0			
3			Autumn (Nov. 2013)	$\text{PM}_{2.5}$	6.8 ± 4.5	15.5 ± 13.4	2.8 ± 2.9	12.7 ± 12.2			
4			Winter (Dec. 2013–Jan. 2014)	$\text{PM}_{2.5}$	13.7 ± 9.8	27.3 ± 29.0	7.3 ± 6.2	35.2 ± 45.6			
5	Shanghai	urban	Jul.–Aug. 2013	$\text{PM}_{1.8}$	2.5 ± 1.3	8.9 ± 6.1	15.7 ± 7.9	11.5 ± 17.4		(Tao et al., 2016)	
6				PM_{10}	2.6 ± 1.3	9.9 ± 6.9	20.1 ± 10.7	15.7 ± 26.4			
7	Shanghai	urban	Jan. 2013	$\text{PM}_{2.5}$	2.4			0.2		(Huang et al., 2016)	
8			Jul.–Aug. 2013	$\text{PM}_{2.5}$	3.9			0.3			
9	Yangzhou	urban	Nov. 2015–Apr. 2016	$\text{PM}_{2.5}$	4.9 ± 1.9	4.3 ± 2.4		15.4 ± 8.1		(Shen et al., 2017)	
10	Nanjing	urban	Apr.–May 2016	$\text{PM}_{2.5}$	7.6	4.2		21.7			
11			Aug. 2014	$\text{PM}_{1.8}$	7.2 ± 4.1	18.0 ± 11.7		36.4 ± 18.6			
12	Xi'an	urban	Jul. 2008–Aug. 2009	$\text{PM}_{2.5}$	14.4 ± 9.6						
13	Guangzhou	urban	Sep.–Oct. 2014	$\text{PM}_{0.095}$	4.3 ± 1.1	41.8 ± 11.4	14.5 ± 3.2	3.7 ± 0.9		(Ho et al., 2015)	
14				PM_5	5.1 ± 1.4	50.4 ± 13.7	17.7 ± 3.6	4.8 ± 1.4		(Liu et al., 2017)	
15				PM_{10}	5.2 ± 1.4	51.8 ± 13.9	19.0 ± 3.8	5.4 ± 1.6			
16	Tampa Bay, Florida	urban	Jul.–Sep. 2005	$\text{PM}_{2.5}$	1.4 ± 1.2	31.6 ± 28.3				(Calderón et al., 2007)	
17	a traffic site, Milan, Italy	urban	Oct. 2013	TSP	4.2 ± 2.9	90 ± 20		360 ± 20		(Perrone et al., 2016)	
18	a limited traffic site, Milan, Italy	urban	Oct. 2013	TSP	4.0 ± 3.0	100 ± 10		420 ± 100			
19	Qingdao	semi-urban	May 2013, Nov.–Dec. 2013, Nov.–Dec. 2015	$\text{PM}_{0.065-10}$		6.3	5.8			(Xie et al., 2018)	
20	resort beach site of Qingdao	coastal, rural	Aug. 2016	$\text{PM}_{0.065-10}$		28.5 ± 23.0	9.0 ± 6.6			(VandenBoer et al., 2012)	
21	Egbert, Toronto	agricultural and semi-forested	Oct. 2010	$\text{PM}_{2.5}$		0.1 ± 0.2	1 ± 0.6				
22	Hyttälä, southern Finland	boreal forest	Mar. 2015	PM_{10}	0.4 ± 0.1	6.8	1.1			(Hemmilä et al., 2018)	
23			Apr. 2015	PM_{10}	0.1 ± 0.1	2.9	0.7				
24			Jul. 2015	PM_{10}	0.1 ± 0.1	3.0	1.8 ± 1.4		0.4		
25	Nanling, Guangdong	forest	Oct. 2016	$\text{PM}_{2.5}$	0.9 ± 0.6	8.8 ± 7.8	1.1 ± 1.8			(Liu et al., 2018a)	
26			May–Jun. 2017		1.8 ± 1.6	11.9 ± 9.8	1.7 ± 1.7				



No.	Site	Site type	Sampling period	Particle size	NH ₄ ⁺ (µg m ⁻³)	Ammonium (ng m ⁻³)				Reference
						MMAH ⁺	DMAH ⁺	TMDEAH ⁺	MEA H ⁺	
27	Huaniao Island	marine	Aug. 2016	PM _{2.5}	0.7±0.4	4.0±0.6	8.7±3.7	< DL	< DL	this study
28			Nov.–Dec. 2016	PM _{1.8}	1.9±1.5	10.7±9.3	6.0±6.8	< DL	< DL	
29				PM ₁₀	2.1±1.8	15.1±12.4	8.4±8.8	< DL	< DL	
30			Mar. 2017	PM _{1.8}	2.0±1.2	6.8±4.6	2.7±1.8	< DL	< DL	
31				PM ₁₀	2.3±1.4	11.4±11.6	3.1±2.2	< DL	< DL	
32			Jun.–Jul. 2017	PM _{1.8}	2.1±1.4	29.0±10.8	24.8±5.4	< DL	< DL	
33				PM ₁₀	2.2±1.6	32.2±11.0	27.5±5.7	< DL	< DL	
34			Aug.–Sep. 2017	PM _{1.8}	1.4±0.7	25.8±8.7	25.0±11.0	< DL	< DL	
35				PM ₁₀	1.5±0.8	27.4±9.1	26.3±11.6	< DL	< DL	
36	the Yellow Sea and the East China Sea	marine	Mar.–Apr. 2017	PM _{1.8}	2.8±2.0	11.9±9.0	14.6±12.9	< DL	< DL	
37				PM ₁₀	3.0±2.2	13.5±10.1	16.6±14.5	< DL	< DL	(Xie et al., 2018)
38	the Yellow Sea and the northwest Pacific	marine	Apr. 2015	PM _{0.056-10}		12.9±10.6	13.2±13.8			
39	the East China Sea	marine	Jan. 2016	PM _{0.056-10}		30.8±9.7	12.0±6.6			
40	the Yellow Sea and the Bohai Sea	marine	Aug. 2015, Jun.–Jul. 2016	PM _{0.056-10}		33.3	19.4			
41	the south Yellow Sea	marine	Nov. 2013	PM _{0.056-10}		18.9±16.6	31.8±19.2			
42	the Yellow Sea and the Bohai Sea	marine	May 2012	PM ₁₁		202±170	432±426			(Hu et al., 2015)
43	the south Yellow Sea	marine	Nov. 2012	PM ₁₀		13.3±4.6	30.0±12.6			(Yu et al., 2016)
44	the north Yellow Sea and the Bohai Sea	marine	Nov. 2012	PM ₁₀		-	15.0±6.6			
45	Arabian Sea	marine	Aug.–Oct. 1994	PM _{0.9}	0.04	2.1	0.3			(Gibb et al., 1999)
46			Nov.–Dec. 1994	PM _{0.9}	0.1	11.1	0.5			
47	Mace Head	marine	Jan.–Dec. 2006	PM ₁		4.7±6.0	7.6±9.4			(Faechini et al., 2008)
48	Irish West Coast	marine	Jun.–Jul. 2006	PM ₁		14.7±14.3	14.3±8.7			
49	the island of São Vicente in Cape Verde	marine	May–Jun., Dec. 2007	PM _{0.1+0.42}	0.1	0.4	0.2			(Müller et al., 2009)
50	off the Central Coast of California	marine	Jul. 2007	PM ₁			22			(Sorooshian et al., 2009)
51	the Eastern Mediterranean	marine	2005–2006	PM ₁		9.2±36.8	< DL			(Violaki and Mihalopoulos, 2010)

631 **Table 3.** Calculated terrestrial and marine source contributions to aminiums over Huaniao Island.

Campaign	DMAH ⁺		TMDEAH ⁺	
	Terrestrial contribution (%)	Marine contribution (%)	Terrestrial contribution (%)	Marine contribution (%)
2016-autumn	71.2 (59.6–81.9)	28.8 (18.1–40.4)	61.6 (25.1–87.4)	38.4 (12.6–74.9)
2017-early summer	42.7 (30.5–54.7)	57.3 (45.3–69.5)	20.9 (5.8–39.1)	79.1 (12.6–94.2)
2017-late summer	33.8 (24.2–45.4)	66.2 (54.6–75.8)	17.5 (4.9–32.9)	82.5 (67.1–95.1)

632